Lucian ION

Solid State Physics

– Laboratory Manual –

May 20, 2014

Preface

0.1 Laboratory procedure

Make sure you have read the experimental and instrumental instructions before coming to the class. You are expected to take all classes, except for some special emergency circumstances. If you are not able to attend the class, inform your instructor to search for an alternative.

All experimental results should be documented in your laboratory notebook. A lab report (which is due in the week that follows from the date you have performed the experiment) will be required for each experiment. You should prepare your own lab report! The structure of the report will be the following:

- The title of the report, your name and the date.
- Abstract: a brief description of the experiment you have performed and of the results you got.
- Theory and methods: succint presentation of the theoretical basis of the project and of the methods you have used to record and interpret experimental data.
- Results section: present your results. Use tables and graphs. Use computer programs (e.g. gnuplot or qtiplot which are available under GNU License) to plot your graphs. Explain the calculations you have performed. Evaluate the errors. Discuss your findings.
- Conclusions: present your main conclusions and suggest possible improvements.
- References: cite any references you have used. Use the format:
  1. A. Einstein, B. Podolsky, N. Rosen, Phys. Rev. **47**, 777 (1935).
  2. N.W. Ashcroft, N.D. Mermin, Solid State Physics (Harcourt, 1976), chapt. 3.

Contents

1

Crystalline structures

1.1 Theory

A crystalline structure or a crystal is a periodic arrangement in space of atoms or groups of atoms. The atom or the group of atoms that is repeated periodically is called *the basis* of the crystalline structure. The set of points in space corresponding to basis locations in a crystal is called *crystalline lattice*. From the very definition of the crystalline structures, it follows that the crystalline lattice is defined as:

$$\mathbf{R}_{n_1 n_2 n_3} = n_1\mathbf{a}_1 + n_2\mathbf{a}_2 + n_3\mathbf{a}_3, \tag{1.1}$$

where the set $\mathbf{a}_1, \mathbf{a}_2, \mathbf{a}_3$ (called the set of *fundamental vectors*) contains the basic periods in the 3D space and $n_i \in \mathbb{Z}$, $|n_i| < N_i/2\, i = 1, 2, 3$, N_i being the number of periods along $\mathbf{a}_i$ direction. Since the interatomic distances in crystals are in the range $3 - 10$ $\mathring{A}$, N_i's are big numbers in macroscopic crystals, a commonly used model consists in extending the crystalline lattice to fill the entire space by replicating the initial crystal with lengths $L_i = N_i a_i,\ i = 1, 2, 3$ over directions of fundamental vectors $\mathbf{a}_i$. Therefore, in this model, $n_i,\ i = 1, 2, 3$ in eq. (1.1) take all integer values. The vectors (1.1) pointing to the sites of the crystalline lattice are called Bravais vectors, after the name of the French physicist Auguste Bravais who studied and classified crystalline structures. The branch of physics concerned with determining the arrangement of atoms in the crystalline solids is called *crystallography*.

The parallelepiped generated by the fundamental vector is called *primitive cell*. A primitive cell contains all the atoms in exactly one basis. The volume of the primitive cell is given by:

$$V_p = |\mathbf{a}_1 \cdot (\mathbf{a}_2 \times \mathbf{a}_3)| = \begin{vmatrix} a_{1x} & a_{1y} & a_{1z} \\ a_{2x} & a_{2y} & a_{2z} \\ a_{3x} & a_{3y} & a_{3z} \end{vmatrix} \tag{1.2}$$

where a_{ix}, a_{iy}, a_{iz} are the components of $\mathbf{a}_i$ in the orthogonal coordinate system (x, y, z).

1.1.1 Crystalline lattice. Translational symmetry

The following notations are used in crystallography:

- a site is defined by the integers in the Bravais vector pointing to it, as $[[n_1 n_2 n_3]]$;
- a direction is defined by the site next to the chosen origin along it, as $[n_1 n_2 n_3]$. Since all the sites are equivalent, any of them may be chosen as the origin of the coordinate system.
- all the sites in a crystalline lattice are distributed in families of parallel planes. Those planes are defined by indicating a set of integers associated to their normal vectors, called Miller's indexes, as (h, k, l). Miller's indexes will be defined below.

To each crystalline lattice in the real, physical, space we will associate its *reciprocal lattice*, as the lattice defined by the fundamental vectors:

$$\mathbf{b}_1 = \frac{2\pi}{V_p}\mathbf{a}_2 \times \mathbf{a}_3 \tag{1.3}$$

$$\mathbf{b}_2 = \frac{2\pi}{V_p}\mathbf{a}_3 \times \mathbf{a}_1 \tag{1.4}$$

$$\mathbf{b}_3 = \frac{2\pi}{V_p}\mathbf{a}_1 \times \mathbf{a}_2. \tag{1.5}$$

All the sites in the reciprocal lattice are then defined by $\mathbf{Q}_{s_1 s_2 s_3} = s_1\mathbf{b}_1 + s_2\mathbf{b}_2 + s_3\mathbf{b}_3$, with $s_i \in \mathbb{Z}$. As a_i is a distance in the physical space, one can easily verify from eqs. (1.3,1.4,1.5) that b_i is the reciprocal of a distance. i.e. it is a wave vector. The reciprocal space is the space of wave vectors.
In addition, from eqs. (1.3,1.4,1.5) it is easily verified that:

$$\mathbf{a}_i \cdot \mathbf{b}_j = 2\pi\delta_{ij}. \tag{1.6}$$

Let's consider an *arbitrary* point in the physical space $\mathbf{r} = x_1\mathbf{a}_1 + x_3\mathbf{a}_2 + x_3\mathbf{a}_3$ and take the scalar product with a vector $\mathbf{Q}_{hkl} = h\mathbf{b}_1 + k\mathbf{b}_2 + l\mathbf{b}_3$ of the reciprocal lattice (h, k, l are integers). Using eq. (1.6) one obtains:

$$\mathbf{Q}_{hkl} \cdot \mathbf{r} = 2\pi(hx_1 + kx_2 + lx_3). \tag{1.7}$$

Recall that the equation of a plane with normal $\mathbf{n}$ and containing the point $\mathbf{r}_0$ is $\mathbf{n} \cdot (\mathbf{r} - \mathbf{r}_0) = 0$. Then eq. (1.7) with variables (x_1, x_2, x_3) defines a plane with $\mathbf{Q}_{hkl}$ directed along its normal (Fig.1.1). Values h, k, l are Miller's indexes of the plane.

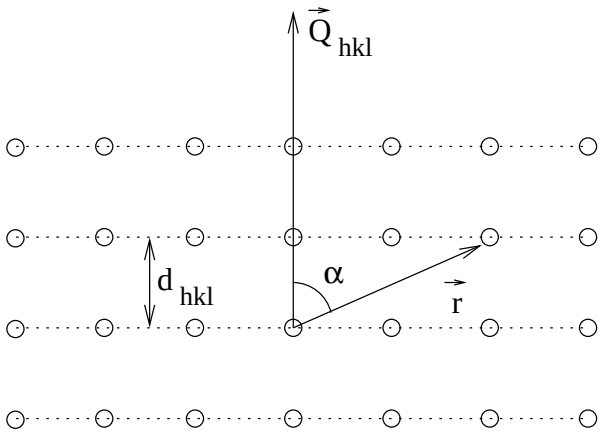

Fig. 1.1. Family of (hkl) planes in a crystalline lattice.

If x_1, x_2, x_3 are integers, then $\mathbf{r}$ is a Bravais vector. For the plane passing through the chosen origin, eq. (1.7) is $\mathbf{Q}_{hkl} \cdot \mathbf{r} = 2\pi(hx_1 + kx_2 + lx_3) = 0$, while for the very next plane in the family along $\mathbf{Q}_{hkl}$ direction it reads $\mathbf{Q}_{hkl} \cdot \mathbf{r} = Q_{hkl}d_{hkl} = 2\pi$, where $d_{hkl} = r\cos\alpha$ is the distance between planes and Q_{hkl} is the magnitude (modulus) of $\mathbf{Q}_{hkl}$. In establishing the last equation it was taken into account that the expression $hx_1 + kx_2 + lx_3$ is an integer taking the successive values $0, 1, \ldots$ for the planes passing through the origin, the next one, etc. It follows that the distance between (h, k, l) planes is given by:

$$d_{hkl} = \frac{2\pi}{Q_{hkl}}. \tag{1.8}$$

As in general vectors $\mathbf{b}_1, \mathbf{b}_2, \mathbf{b}_3$ are not orthogonal, Q_{hkl} is given by:

$$Q_{hkl} = \sqrt{h^2 b_1^2 + k^2 b_2^2 + l^2 b_3^2 + 2hk\cos(\mathbf{b}_1\hat{,}\mathbf{b}_2) + 2kl\cos(\mathbf{b}_2\hat{,}\mathbf{b}_3) + 2hl\cos(\mathbf{b}_3\hat{,}\mathbf{b}_1)}. \tag{1.9}$$

A change in coordinates or variables of an object which leaves it invariant, is called a *symmetry transformation* of that object. Let $\hat{O}$ be the *symmetry operation* describing the change of the coordinates associated to a geometric symmetry transformation taking the point $\mathbf{r}$ to the point $\mathbf{r}' = \hat{O}\mathbf{r}$ (relative to a *fixed coordinate system*) and $f(\mathbf{r})$ an arbitrary physical property of the object (e.g. the charge density of a crystal). The invariance of the properties of the object is mathematically expressed as $f(\mathbf{r}') = f(\hat{O}\mathbf{r}) = f(\mathbf{r})$.

The fundamental symmetry of a crystalline lattice, deriving from its definition in eq. (1.1), is its invariance to translations defined by Bravais vectors, i.e. $\mathbf{r}' = T_{\mathbf{R}}\mathbf{r} = \mathbf{r} + \mathbf{R}_{n_1 n_2 n_3}$. Since two successive translations by Bravais vectors $\mathbf{R}_1$ and $\mathbf{R}_2$ is a translation by Bravais vector $\mathbf{R}_1 + \mathbf{R}_2$, the following properties are easily verified, based on the mathematical properties of the addition of vectors:

- associativity of translations by Bravais vectors: $T_{\mathbf{R}_1}(T_{\mathbf{R}_2}T_{\mathbf{R}_3}) = (T_{\mathbf{R}_1}T_{\mathbf{R}_2})T_{\mathbf{R}_3} = T_{\mathbf{R}_1}T_{\mathbf{R}_2}T_{\mathbf{R}_3} = T_{\mathbf{R}_1+\mathbf{R}_2+\mathbf{R}_3}$, $(\forall)T_{\mathbf{R}_1}, T_{\mathbf{R}_2}, T_{\mathbf{R}_3}$;
- commutativity of translations by Bravais vectors: $T_{\mathbf{R}_1}T_{\mathbf{R}_2} = T_{\mathbf{R}_2}T_{\mathbf{R}_1}$, $(\forall)T_{\mathbf{R}_1}, T_{\mathbf{R}_2}$;
- identity element: $T_{\mathbf{0}}T_{\mathbf{R}} = T_{\mathbf{R}}T_{\mathbf{0}} = T_{\mathbf{R}}$, $(\forall)T_{\mathbf{R}}$;
- inverse element: $(\forall)T_{\mathbf{R}}$, $(\exists)T_{\mathbf{R}}^{-1} = T_{-\mathbf{R}}$, with $T_{\mathbf{R}}T_{\mathbf{R}}^{-1} = T_{\mathbf{R}}^{-1}T_{\mathbf{R}} = T_{\mathbf{0}}$.

It follows that the infinite set of Bravais translations $\{T_{\mathbf{R}}\}$ with the internal composition law introduced above is organised as an abelian group. Translational invariance of the crystalline lattice is related to the *long range order* in crystals.

1.1.2 Point symmetry. Crystal classes.

A symmetry transformation which brings a body into coincidence with itself while keeping at least one of its points fixed, is called a point symmetry. Examples:

- Rotation about an axis: suppose that the rotation axis is Oz and the rotation angle is φ. Then the change in coordinates is given by the rotation matrix:

$$\begin{pmatrix} x' \\ y' \\ z' \end{pmatrix} = \begin{pmatrix} \cos\varphi & -\sin\varphi & 0 \\ \sin\varphi & \cos\varphi & 0 \\ 0 & 0 & 1 \end{pmatrix} \cdot \begin{pmatrix} x \\ y \\ z \end{pmatrix} \tag{1.10}$$

  If the rotation angle is $\varphi = \frac{2\pi}{n}$, the notation for the rotation symmetry element is n (n-fold rotational symmetry). This is the international crystallographic notation (or Hermann-Mauguin notation).
- Reflection in a plane: suppose the mirror is xy plane. Then the change in coordinates is given by the matrix:

$$\begin{pmatrix} x' \\ y' \\ z' \end{pmatrix} = \begin{pmatrix} 1 & 0 & 0 \\ 0 & 1 & 0 \\ 0 & 0 & -1 \end{pmatrix} \cdot \begin{pmatrix} x \\ y \\ z \end{pmatrix} \tag{1.11}$$

  The notation for the reflection symmetry element is m (mirror).
- Spatial inversion (the notation is i):

$$\begin{pmatrix} x' \\ y' \\ z' \end{pmatrix} = \begin{pmatrix} -1 & 0 & 0 \\ 0 & -1 & 0 \\ 0 & 0 & -1 \end{pmatrix} \cdot \begin{pmatrix} x \\ y \\ z \end{pmatrix} \tag{1.12}$$

- Rotoinversion or rotary inversion[1]: rotation about an axis, followed by an inversion about a point on the axis. This is a new point symmetry: the analyzed object is not invariant by rotation or inversion only. If

[1] Another possible choice for this supplemental point symmetry would be the rotoreflection or rotary reflection: a rotation followed by a reflection in a plane perpendicular to the rotation axis. This type of point symmetry is used in physics of molecules. In crystallography, the rotary inversion is preferred, being more suitable.

the rotation angle is $\varphi = \frac{2\pi}{n}$, the Hermann-Mauguin notation for the rotation-inversion symmetry element is $\overline{n}$. If the rotation axis is Oz, the change in coordinates is given by:

$$\begin{pmatrix} x' \\ y' \\ z' \end{pmatrix} = \begin{pmatrix} -\cos\varphi & \sin\varphi & 0 \\ -\sin\varphi & -\cos\varphi & 0 \\ 0 & 0 & -1 \end{pmatrix} \cdot \begin{pmatrix} x \\ y \\ z \end{pmatrix}. \tag{1.13}$$

Let A be the matrix describing a point symmetry element. If $\det A = +1$, the symmetry element is called *proper* (it transforms a right-handed trihedron into a right-handed trihedron). If $\det A = -1$, the symmetry element is called *improper* (it transforms a right-handed trihedron into a left-handed trihedron). Pure rotations are the only proper point symmetry elements.

The point symmetry of crystalline structures must be compatible to their fundamental property, which is the long range order (translational symmetry). Suppose that a crystalline lattice is invariant by rotation about an axis and let φ be the rotation angle (Fig. 1.2).

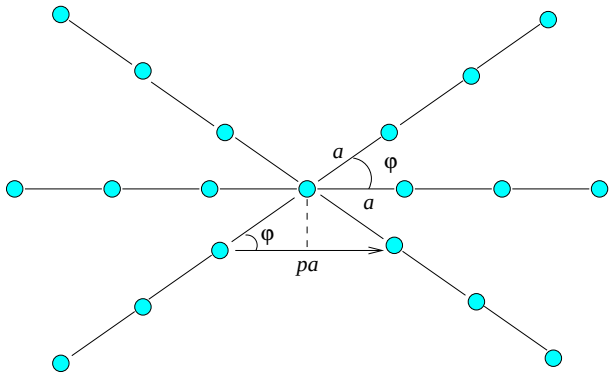

Fig. 1.2. Transformation of a crystalline lattice after rotation about an axis perpendicular to the plane of the figure.

Let a be the distance between first neighbour sites in one row of the lattice. The rotations of the selected row by $\pm\varphi$ result in the configuration plotted in Fig. 1.2. Since a is the smallest distance between sites on the selected row, the distance between sites indicated by the arrow must be an integer multiple of a:

$$pa = 2a\cos\varphi. \tag{1.14}$$

It follows that $\cos\varphi = \frac{p}{2},\ p \in \mathbb{Z}$ and

$$-1 \leq \frac{p}{2} \leq 1. \tag{1.15}$$

All the possible values for the integer p and the rotation angle φ are listed in Table 1.1.

Table 1.1. Rotations compatible with translational symmetry of crystalline lattices.

p	φ	n-fold axis
-2	π	2
-1	$\frac{2\pi}{3}$	3
0	$\frac{\pi}{2}$	4
1	$\frac{\pi}{3}$	6
2	2π	1

A crystalline structure can only be invariant by the following rotations or rotary inversions: $1, \overline{1}, 2, \overline{2}, 3, \overline{3}, 4, \overline{4}, 6, \overline{6}$. It is easy to show that $\overline{1} = i$ and $\overline{2} = m$ (left as an exercise).
All point symmetry elements of a crystalline structure form a group: the *point group* of the structure. The identity element is 1 (rotation by 2π).
The simplest groups that can be generated by the allowed point symmetry elements are $\{1\}$ and $\{1, i\}$. The corresponding primitive cell is an parallelepiped whose faces are arbitrary parallelograms, i.e. $a_1 \neq a_2 \neq a_3 \neq a_1$ and $\alpha_{12} \neq \alpha_{23} \neq \alpha_{31} \neq \alpha_{12}$, where $\alpha_{ij} \neq \frac{\pi}{2}$ is the angle between $\mathbf{a}_i$ and $\mathbf{a}_j$. These crystalline structures belong to the less-symmetric class or syngony, called *triclinic*. Only simple (or primitive) structures exist in this class, i.e. all the sites are in the vertices of the unit cell.
Next are the groups containing a single 2-fold axis or a mirror, i.e. $\{1, 2\}$, $\{1, m\}$ and $\{1, 2, m, i\}$. The corresponding primitive cell is a parallelepiped with two arbitrary parallelograms as bases, the lateral faces being rectangles: $a_1 \neq a_2 \neq a_3 \neq a_1$ and $\frac{\pi}{2} = \alpha_{12} = \alpha_{23} \neq \alpha_{31}$. Simple (primitive) and base-centered (sites in the vertices and in the center of parallelogram bases of the unit cell) structures exist in this class. Elemental sulfur is an example of monoclinic crystal (but it can also exist in other forms).
All crystals can be classified based on their point symmetry (Table 1.2).

Table 1.2. Classification of crystalline lattices based on their point symmetry.

Crystal class (syngony)	Unit cell	Type
triclinic	$a_1 \neq a_2 \neq a_3 \neq a_1$, $\alpha_{12} \neq \alpha_{23} \neq \alpha_{31} \neq \alpha_{12}$	primitive
monoclinic	$a_1 \neq a_2 \neq a_3 \neq a_1$, $\frac{\pi}{2} = \alpha_{12} = \alpha_{23} \neq \alpha_{31}$	primitive, base-centered
orthorhombic	$a_1 \neq a_2 \neq a_3 \neq a_1$, $\frac{\pi}{2} = \alpha_{12} = \alpha_{23} = \alpha_{31}$	primitive, base-centered, body-centered, face-centered
rhombohedral or trigonal	$a_1 = a_2 = a_3$, $\frac{\pi}{2} \neq \alpha_{12} = \alpha_{23} = \alpha_{31}$	primitive
tetragonal	$a_1 = a_2 \neq a_3$, $\frac{\pi}{2} = \alpha_{12} = \alpha_{23} = \alpha_{31}$	primitive, body-centered
cubic	$a_1 = a_2 = a_3$, $\frac{\pi}{2} = \alpha_{12} = \alpha_{23} = \alpha_{31}$	primitive, body-centered, face-centered
hexagonal	$a_1 = a_2 \neq a_3$, $\frac{\pi}{2} = \alpha_{13} = \alpha_{23}$, $\frac{2\pi}{3} = \alpha_{12}$	primitive

There are in all 7 crystal classes (or syngonies) and 14 types of lattices. The body-centered type unit cell has sites in the vertices and in its center of mass. The face-centered type unit cell has sites in the vertices and in the center of its faces. The base-centered type unit cell has sites in the vertices and in the center of its bases. Point symmetry elements transform a crystalline direction into an equivalent one. It is the symmetry of material tensors (e.g. electrical conductivity, permitivity, etc.)

1.1.3 Space symmetry. Space groups

The complete symmetry of a crystalline structure is obtained by combining translations $T_{\mathbf{t}}$ with point symmetry elements r, to obtain *space symmetry* elements:

$$g = T_{\mathbf{t}}\, r = (r|\mathbf{t}). \tag{1.16}$$

The composition law of two space symmetry elements is given by:

$$g_1 g_2 = T_{\mathbf{t}_1}\, r_1 T_{\mathbf{t}_2}\, r_2 = (r_1 r_2 | \mathbf{t}_1 + r_1 \mathbf{t}_2). \tag{1.17}$$

The translation associated to a given point symmetry element is defined by eq. (1.17), starting from the translations of the generators of the point group. In general, $\mathbf{t}$ is not a Bravais vector:

$$\mathbf{t} = \mathbf{R} + \boldsymbol{\rho}. \tag{1.18}$$

with $\boldsymbol{\rho} = \gamma_1 \mathbf{a}_1 + \gamma_2 \mathbf{a}_2 + \gamma_3 \mathbf{a}_3$, $|\gamma_i| < 1$. Values $\gamma_i \neq 0$ are always associated to a complex basis of the crystalline structure, containing more than one chemically equivalent atoms.

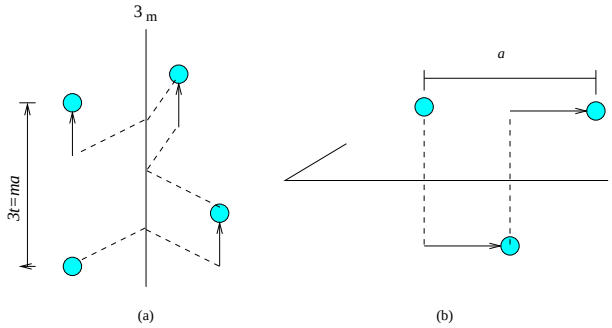

Fig. 1.3. Space symmetry elements: screw axis (a) and glide mirror (b).

Space symmetry elements generated as stated above are *screw axes* (or helical axes) and *glide mirrors* (Fig. 1.3). Screw axes and glide mirrors with $\boldsymbol{\rho} \neq \mathbf{0}$ are called *essential*.

The set of space symmetry operations with the composition law (1.17) forms a group: *the space group* of the crystal. There are 230 space groups. If a space group contains essential screw axes or glide mirrors, it is called *non-symmorphic*. Otherwise, it is called *symmorphic*. There are 77 symmorphic space groups. Space symmetry is the microscopic symmetry of the crystals; it is the symmetry of wave-functions.

1.2 Experimental setup and procedure

You are asked to perform a geometrical characterization of selected crystalline structures. Use the models available in lab. The procedure you will follow is indicated below, in the case of a body-centered cubic (bcc) structure (Fig. 1.4). Iron has this type of structure.

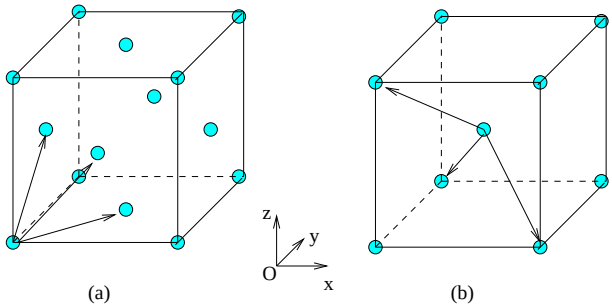

Fig. 1.4. Face-centered cubic (a) and body-centered cubic (b) unit cells. Fundamental translation vectors are indicated in both cases.

- *Search for fundamental translation vectors. Give their expressions, relative to an orthogonal coordinate system.* [2]
  For the bcc structure the fundamental translation vectors are:

[2] **Hint**: search for three linear-independent vectors conecting first neighbour sites in the structure. Use the symmetry of the structure. Make sure that all sites can be obtained using eq. (1.1) based on the fundamental vectors you have selected.

$$\mathbf{a}_1 = \frac{a}{2}(\mathbf{x} - \mathbf{y} - \mathbf{z}) \tag{1.19}$$

$$\mathbf{a}_2 = \frac{a}{2}(-\mathbf{x} + \mathbf{y} - \mathbf{z}) \tag{1.20}$$

$$\mathbf{a}_3 = \frac{a}{2}(-\mathbf{x} - \mathbf{y} + \mathbf{z}), \tag{1.21}$$

a being the edge of the cube. The primitive cell is a rhombohedron, generated by the fundamental vectors. Its volume is (see eq. (1.2))

$$V_p = |\mathbf{a}_1 \cdot (\mathbf{a}_2 \times \mathbf{a}_3)| = \frac{a^3}{8}\begin{Vmatrix} 1 & -1 & -1 \\ -1 & 1 & -1 \\ -1 & -1 & 1 \end{Vmatrix} = \frac{a^3}{2}. \tag{1.22}$$

However, bcc and fcc structures are not chracterized in crystallography by the primitive cells. The reason is the fact that the maximum symmetry of the primitive cell (the rhombohedron) is 3, while the maximum symmetry of the cubic structure is 4. In these two cases, 4-fold axes are generated by packaging of rhombohedra with peculiar angles between fundamental vectors. Instead, the cubic unit cell is used, as it contains all point symmetry elements of the structure. The unit cell vectors are simply:

$$\mathbf{c}_1 = a\mathbf{x} \tag{1.23}$$

$$\mathbf{c}_2 = a\mathbf{y} \tag{1.24}$$

$$\mathbf{c}_3 = a\mathbf{z}. \tag{1.25}$$

The volume of the unit cell is $V = a^3$. The *multiplicity* of the unit cell is defined as $M = \frac{V}{V_p} = 2$. The bcc unit cell is twice the primitive cell.
The unit cell of the bcc structure contains two *equivalent* sites (each one can be obtained from the other by a Bravais fundamental translation): $[[000]]$, $[[\frac{1}{2}\frac{1}{2}\frac{1}{2}]]$. This is because its multiplicity is 2. In general, the number of atoms in a unit cell can be calculated as:

$$N = \frac{1}{8}N_v + \frac{1}{6}N_f + \frac{1}{4}N_e + N_i, \tag{1.26}$$

where N_v is the number of atoms in vertices of the cell, N_f is the number of atoms on the faces, N_e is the number of atoms on the edges and N_i is the number of atoms inside the cell.
Relative to the cubic vectors, generating the unit cell, all the sites of the structure can be described as $[[u, v, w]]$, $[[u + \frac{1}{2}, v + \frac{1}{2}, w + \frac{1}{2}]]$, with $u, v, w \in \mathbb{Z}$. From this point on, all reference is to cubic vectors (1.25).

- *Search for the first and second neighbours to a given atom.*
  This is important, because in general the electronic structure of crystals is determined by interactions between first and second neighbours. The number of first neighbours in bcc structure is 8 and the distance between them is $\frac{a\sqrt{3}}{2}$. The number of second neighbours is 6 and the distance between them is a.
- *Suppose that first neighbours are rigid spheres. The fill factor is defined as the ratio of the volume occupied by the spheres to the total volume of the structure. Evaluate the fill factor. Evaluate the radius of the largest sphere (this could be an impurity atom) that can be introduced in the structure in an empty space, without deforming the structure.*
  The distance between first neighbours is twice the radius of a sphere, so $R = \frac{a\sqrt{3}}{4}$. As in the unit cell there are two complete spheres, the fill factor is $k = \frac{2\frac{4\pi}{3}R^3}{a^3} = \frac{\sqrt{3}\pi}{8} \approx 0.68$.
- *Identify the point symmetry elements.*
  - 3 4-fold rotations: [100], [010], [001];
  - 4 3-fold rotations: [111], $[\overline{1}\,\overline{1}1]$, $[1\overline{1}1]$, $[\overline{1}11]$;
  - 6 2-fold rotations: [110], $[\overline{1}10]$, [101], $[\overline{1}01]$, [011], $[0\overline{1}1]$;
  - 3 mirrors: (100), (010), (001);
  - 6 mirrors: (110), $(1\overline{1}0)$, (101), $(10\overline{1})$, (011), $(01\overline{1})$;
  - inversion.

- *Determine the reciprocal lattice. Give the general expression for interplanar distance.*
  Reciprocal basis vectors are:

$$\mathbf{b}_1 = \frac{2\pi}{V}\mathbf{c}_2 \times \mathbf{c}_3 = \frac{2\pi}{a}\mathbf{x} \tag{1.27}$$

$$\mathbf{b}_2 = \frac{2\pi}{V}\mathbf{c}_3 \times \mathbf{c}_1 = \frac{2\pi}{a}\mathbf{y} \tag{1.28}$$

$$\mathbf{b}_3 = \frac{2\pi}{V}\mathbf{c}_1 \times \mathbf{c}_2 = \frac{2\pi}{a}\mathbf{z}. \tag{1.29}$$

  and they seem to generate a cubic lattice. However, there is a constraint on the points generated by the above determined vectors: since $\mathbf{c}_1, \mathbf{c}_2, \mathbf{c}_3$ are not fundamental Bravais translations, $\mathbf{Q}_{hkl} = h\mathbf{b}_1 + k\mathbf{b}_2 + l\mathbf{b}_3$ is a vector of the reciprocal lattice if and only if $\mathbf{Q}_{hkl} \cdot \mathbf{R}_c = 2\pi p$, $p \in \mathbb{Z}$, with $\mathbf{R}_c = u\mathbf{c}_1 + v\mathbf{c}_2 + w\mathbf{c}_3$ or $\mathbf{R}_c = \left(u + \frac{1}{2}\right)\mathbf{c}_1 + \left(v + \frac{1}{2}\right)\mathbf{c}_2 + \left(w + \frac{1}{2}\right)\mathbf{c}_3$, $u, v, w \in \mathbb{Z}$. Since $\mathbf{c}_i \cdot \mathbf{b}_j = 2\pi\delta_{ij}$, the following equations are obtained:

$$hu + kv + lw = p_1 \tag{1.30}$$

$$h\left(u + \frac{1}{2}\right) + k\left(v + \frac{1}{2}\right) + l\left(w + \frac{1}{2}\right) = p_2 \tag{1.31}$$

  with $p_{1,2} \in \mathbb{Z}$. This is true when $h, k, l \in \mathbb{Z}$ and $\frac{h+k+l}{2} \in \mathbb{Z}$. It is easily verified that these two conditions define a fcc lattice. So, the reciprocal lattice of the bcc lattice is a fcc one. The reciprocal statement is also true: the reciprocal lattice of the fcc is a bcc one.[3].
  The distance between (hkl) planes is given by (1.8):

$$d_{hkl} = \frac{2\pi}{Q_{hkl}} = \frac{a}{\sqrt{h^2 + k^2 + l^2}}. \tag{1.32}$$

  Recall that h, k, l are subject to above determined constraints.

1.3 Tasks

Use the procedure described above to characterize the following two crystalline structures:
- the fcc crystalline structure;
- the hexagonal compact (hc) crystalline structure.

The two mentioned structures are related, although their point groups are very different. Try to understand why.

[3] One can easily check that the same result is obtained if the fundamental vectors $\mathbf{a}_1, \mathbf{a}_2, \mathbf{a}_3$ are used instead of cubic ones.

2

Investigation of copper crystalline structure by X-ray diffraction

Interatomic distances in crystalline solids are tipically in the range $3 - 10$ $\mathring{A}$. The periodic three-dimensional lattice of a crystal diffracts electromagnetic radiation with suitable wavelength the same way a ruled diffraction grating diffracts the visible light. The electromagnetic radiation suitable for investigating structural properties of crystals should have wavelengths in the range $0.5 - 2.0$ $\mathring{A}$. This is in the X-ray region of the electromagnetic spectrum.

2.1 Theory

X-ray beams used in crystallography are produced in X-ray tubes or in synchrotrons. Obviously the first type of source is by far less expensive and most used in modern diffractometers. Synchrotron radiation is rather used in special more advanced applications.

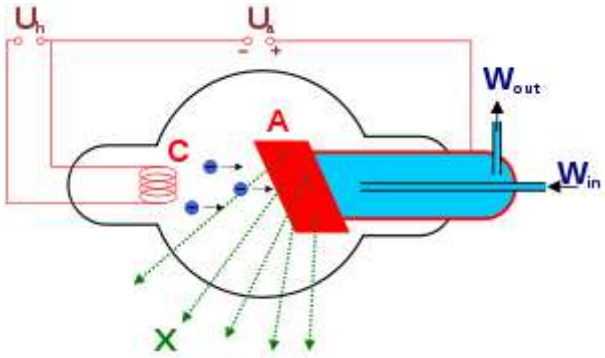

Fig. 2.1. Schematics of a X-ray tube.

In a X-ray tube (Fig. 2.1) electrons accelerated to energies of tens keV, emitted by a hot cathode, are directed towards a metallic anticathode (or anode), usually water-cooled. Due to Coulomb interactions with the electrons and nuclei of the anticathode material, X-rays are emitted, The typical emission spectrum is shown in figure 2.2.

The continuous part of the spectrum is due to electrons which are suddenly decelerated upon collision with the metal target (*brehmsstralung*). It is independent of the anticathode material. The minimum wavelength depends on the initial kinetic energy of electrons (i.e. the high voltage applied between cathode and anticathode):

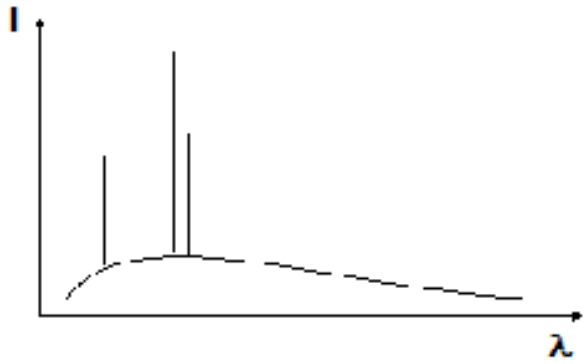

Fig. 2.2. Typical emission spectrum of a X-ray tube.

$$\lambda_{min} = \frac{12400}{U(V)} \, \mathring{A}. \tag{2.1}$$

Characteristic X-rays depends on the anticathode material; if the bombarding electrons have sufficient energy, they can excite an electron from an inner shell n of the target metal atoms. Then electrons from higher states n_1 drop down to fill the vacancy, emitting X-ray photons with determined energies $E_{n_1} - E_n$, set by the electron energy levels. Figure 2.3 shows the series of emission lines; some of the most used in crystallography are collected in table 2.1.

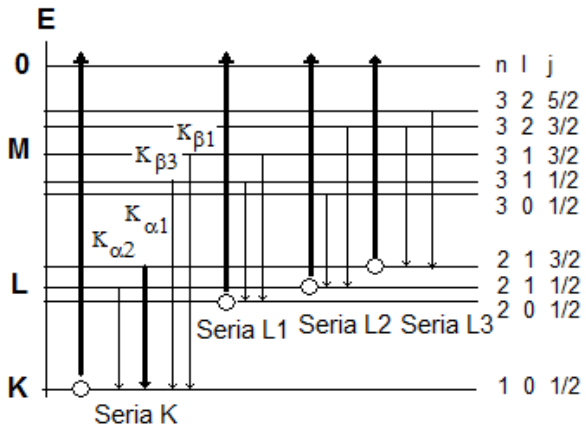

Fig. 2.3. Characteristic X-rays emited in a X-ray tube. Selection rules are: $\Delta l = \pm 1, \ \Delta j = 0, \pm 1$.

Table 2.1. Spectral emission lines for some of the most used anticathode materials.

Element	K_{β_1} ($\mathring{A}$)	K_{α_1} ($\mathring{A}$)	K_{α_2} ($\mathring{A}$)
Mo	0.63225	0.70926	0.71354
Cu	1.39217	1.54059	1.54433
Co	1.62075	1.78892	1.79278
Fe	1.79278	1.93597	1.93991
Cr	2.08479	2.28962	2.29352

One of the most used experimental setups in modern diffractometers is the so-called Bragg-Brentano geometry: the X-ray tube and the elements of the input optics are mounted on one arm of a goniometer, while the output optics and the detector are mounted on the other arm (Fig. 2.4). The sample is stationary while the X-ray tube and the detector are rotated around it. The angle formed between the tube and the detector is 2θ, θ being the angle formed between the direction of the incident X-rays and the surface of the sample. This is the Bragg-Brentano theta-theta geometry.

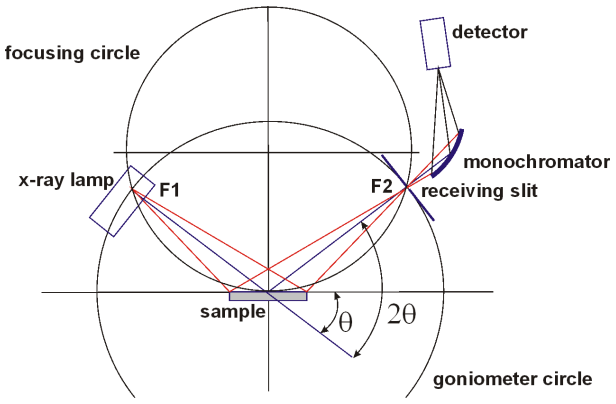

Fig. 2.4. The Bragg-Brentano geometry. The arms of the goniometer are coupled in their rotation, in the way that the diffracted radiation is detected at the scattering angle 2θ, the incident X-rays being directed at the angle θ with respect to the surface of the analyzed sample.

The diffraction pattern recorded in Bragg-Brentano geometry consists of one (in the case of monocrystals) or several peaks (polycrystalline materials or powder) at specific incident angles, defined by Bragg's law:

$$2d_{hkl}\sin\theta = n\lambda, \tag{2.2}$$

d_{hkl} being the distance between (hkl) planes, given by

$$d_{hkl} = \frac{2\pi}{Q_{hkl}}, \tag{2.3}$$

with $\mathbf{Q}_{hkl} = h\mathbf{b}_1 + k\mathbf{b}_2 + l\mathbf{b}_3$, $\mathbf{b}_i,\ i = 1, 2, 3$ being the fundamental translation vectors of the reciprocal lattice. For cubic crystals with lattice constant a:

$$d_{hkl} = \frac{a}{\sqrt{h^2 + k^2 + l^2}}. \tag{2.4}$$

Miller's indexes h, k, l are subject to the following constraints in the case of cubic structures:

- Simple cubic lattice: h, k, l are integers, no supplementary constraints;
- Body-centered cubic lattice: h, k, l are integers and $h + k + l$ is an even integer;
- Face-centered cubic lattice: h, k, l are integers and $h + k, k + l, h + l$ are even.

Observed peaks correspond to reciprocal sites located at the same distance Q to the origin, which is usually a consequence of the point symmetry. Let M be the number of reciprocal sites corresponding to the considered peak (its *multiplicity*). For example, in a simple cubic crystal, (100) peak has $M = 6$, because in a powder diffraction experiments the grains with $(100), (\overline{1}00), (010), (0\overline{1}0), (001), (00\overline{1})$ planes oriented parallel to the surface of the sample contribute to the peak appearing at the same 2θ angle.

2.2 Experimental setup and procedure

This experiment will be performed under the supervision of an authorized person, after a proper training.
The diffraction pattern of a polycrystalline copper sample will be recorded in the 2θ range 10°- 100° by using a diffractometer with $Cu_{K_{\alpha_1}}$ radiation (the corresponding wavelength is in table 2.1). From eq. (2.2) it follows that for cubic structures:

$$\sin^2\theta = \frac{\lambda^2}{4a^2}(h^2+k^2+l^2) \tag{2.5}$$

with $\sin^2\theta$ values ranging in an arithmetc progression (with some missing terms, due to above mentioned constraints, see also table 2.2). The cubic lattice constant a may be determined if the wavelength of the incident monochromatic X-ray beam is known and the peaks are indexed correctly.

Table 2.2. *hkl* Miller's indexes with increasing $h^2+k^2+l^2$ values in cubic crystals.

hkl	Primitive: $h^2+k^2+l^2$	Body-centered (bcc): $h^2+k^2+l^2$	Face-centered (fcc): $h^2+k^2+l^2$
100	1	-	-
110	2	2	-
111	3	-	3
200	4	4	4
210	5	-	-
211	6	6	-
220	8	8	8
221-300	9	-	-
310	10	10	-
311	11	-	11
222	12	12	12
320	13	-	-
321	14	14	-

From data in table 2.2 it follows that the sequence of experimentally obtained $\sin^2\theta$ values, θ being the center of the peak, is proportional to:

- 1 2 3 4 5 6 8 etc. for primitive (simple) cubic crystals;
- 1 2 3 4 5 6 7 etc. for body-centered cubic crystals;
- 1 4/3 8/3 11/3 4 etc. for face-centered cubic crystals.

2.3 Tasks

- Indicate Miller's indexes (hkl) corresponding to each observed peak in the diffraction pattern of the copper sample. Identify the lattice type of the copper crystal. (*Hint*: the lattice is cubic; you have to find out the precise type of cubic lattice. Use the sequence of $\sin^2\theta$ values.);
- Determine the lattice constant a.

3

Temperature dependence of electrical resistivity of metals

3.1 Theory

Charge transport in macroscopic (semi)conductors can be described in the frame of Boltzmann's approach, in the time relaxation approximation. A conductor will respond to an external applied electrical field by establishing a flow of free carriers - an electrical current. The current density, $\mathbf{j}$, will be proportional to the applied field if the field is not too strong:

$$\mathbf{j} = \hat{\sigma} \cdot \mathbf{E}, \tag{3.1}$$

which is the well-known Ohm's law, in its local form.
This is an out-of-equilibrium state of the conductor, described by some one-particle distribution function $f(\mathbf{r}, \mathbf{k}, t)$, expressing the probability to find a charge carrier (e.g. an electron in the conduction band) in the position $\mathbf{r}$, in the state indexed by the wave vector $\mathbf{k}$ at time t.
In thermodynamic equilibrium:

$$\frac{df_0}{dt} = 0, \tag{3.2}$$

with f_0 being Fermi-Dirac distribution function:

$$f_0(\mathbf{k}) = \frac{1}{1 + \exp\left(\frac{E(\mathbf{k}) - E_F}{k_B T}\right)}, \tag{3.3}$$

eq. (3.2) expressing the fact that the electron gas is homogeneous throughout the system and its properties do not depend on time. In (3.3) k_B is Boltzmann's constant.

In the out-of-equilibrium state, the evolution of the distribution function is given by Boltzmann's equation:

$$\frac{df}{dt} = \left(\frac{\partial f}{\partial t}\right)_{coll}, \tag{3.4}$$

or, expressing the total derivative in the left-hand-side:

$$\frac{\partial f}{\partial t} + \mathbf{v} \cdot \nabla_{\mathbf{r}} f - \frac{e}{\hbar} \mathbf{E} \cdot \nabla_{\mathbf{k}} f = \left(\frac{\partial f}{\partial t}\right)_{coll}. \tag{3.5}$$

In eq. (3.5) $\mathbf{v} = \frac{1}{\hbar} \nabla_{\mathbf{k}} E(\mathbf{k})$ is the mean velocity of an electron in a Bloch state with energy $E(\mathbf{k})$ in the conduction band, $\mathbf{F}_e = -e\mathbf{E}$ is the force acting on an electron due to the applied field and the right-hand-side $\left(\frac{\partial f}{\partial t}\right)_{coll}$ is the so-called *collision term*, or *collision integral*, describing the effect of scattering events affecting electron

dynamics, associated to defects inherent in real crystals. These defects break the translational symmetry of a perfect crystal. If the crystalline order is not significantly altered, the potential energy describing electron-defect interaction will act as a small localized (in space and time) perturbation to the one-particle Hamiltonian corresponding to the perfect crystal. Consequently, the dynamics of free charge carriers (e.g. electrons in the conduction band of metals), can be characterized as being a *diffusive* one: the defects will scatter the carriers from one Bloch's state to another in the same band, inducing a *rapid relaxation* of the momentum and/or the energy of the carriers. In *the relaxation time approximation*, one writes:

$$\left(\frac{\partial f}{\partial t}\right)_{coll} = -\frac{f - f_0}{\tau(\mathbf{k})}, \tag{3.6}$$

where f and f_0 are distribution functions out-of-equilibrium and, respectively, in equilibrium, and $\tau(\mathbf{k})$ is the *relaxation time* of the momentum and/or energy. The relaxation time $\tau(\mathbf{k})$ is given by the quantum mechanics of the scattering process associated to a particular scatterer.

We may classify the main scatterers as follows:
- static scatterers: they only scatter free carriers elastically (the momentum of free carriers is changed, their energy being conserved; examples: point-like or extended defects with no internal degrees of freedom);
- dynamic scatterers: they scatter free carriers inelastically (both the energy and momentum are changed; example: electron-phonon interaction, electron-electron interaction, impurities with internal degrees of freedom accessible at typical energies of free carriers).

Suppose that the system of interest is a metallic sample, made of a cubic (isotropic) metal and the applied electric field is stationary (independent of time) and homogeneous (independent of $\mathbf{r}$). Then, except for a small period of time immediately after applying the field, there is no reason for the distribution function to depend on time or position (i.e. we only consider the stationary case). In addition, we will restrict our analysis to the *linear response* only (the conductivity in eq. 3.1 is a linear response function!) by introducing:

$$f(\mathbf{k}) = f_0(\mathbf{k}) + f_1(\mathbf{k}), \tag{3.7}$$

$f_1(\mathbf{k})$ being a function of the first order of the applied field (e.g. $f_1(\mathbf{k}) \propto \mathbf{E}$). Then the linearized Boltzmann's equation (3.5) reads:

$$f_1(\mathbf{k}) = \frac{e}{\hbar}\tau(\mathbf{k})\mathbf{E}\cdot\nabla_{\mathbf{k}} f_0(\mathbf{k}) = e\tau(\mathbf{k})\mathbf{v}\cdot\mathbf{E}\frac{\partial f_0}{\partial E}. \tag{3.8}$$

In writing eq. (3.8) we only kept the terms linear in $\mathbf{E}$ and we have used $\frac{1}{\hbar}\nabla_{\mathbf{k}} f_0(\mathbf{k}) = \frac{1}{\hbar}\nabla_{\mathbf{k}} E(\mathbf{k})\frac{\partial f_0}{\partial E}$, with $\mathbf{v} = \frac{1}{\hbar}\nabla_{\mathbf{k}} E(\mathbf{k})$.

The current density is defined as:

$$\mathbf{j} = \frac{(-e)}{V}\sum_{\mathbf{k},s}\mathbf{v} f(\mathbf{k}) = \frac{(-e)}{V}\sum_{\mathbf{k},s}\mathbf{v} f_1(\mathbf{k}), \tag{3.9}$$

as $\sum_{\mathbf{k},s}\mathbf{v} f_0(\mathbf{k}) = 0$ due to the fact that in summing over the first Brillouin zone $f_0(\mathbf{k}) = f_0(-\mathbf{k})$, while $\mathbf{v} \propto \mathbf{k}$. Passing from summation to integral over the first Brillouin zone (i.e. $\sum_{\mathbf{k}} A(\mathbf{k}) = \frac{V}{(2\pi)^3}\int_{BZ} A(\mathbf{k})d^3k$), the above equation reads (the factor 2 comes from spin degeneracy):

$$\mathbf{j} = \frac{(-2e)}{(2\pi)^3}\int_{BZ}\mathbf{v} f_1(\mathbf{k})d^3k, \tag{3.10}$$

or, using eq. (3.8):

$$\mathbf{j} = \frac{(-2e^2)}{(2\pi)^3}\int_{BZ}\mathbf{v}(\mathbf{v}\cdot\mathbf{E})\tau(\mathbf{k})\frac{\partial f_0}{\partial E}d^3k. \tag{3.11}$$

The above equation is Ohm's law; it follows that j_α component of the current density ($\alpha = x, y, z$) is given by

$$j_\alpha = \frac{(-2e^2)}{(2\pi)^3} \int_{BZ} v_\alpha (\sum_\beta v_\beta E_\beta) \tau(\mathbf{k}) \frac{\partial f_0}{\partial E} d^3k, \tag{3.12}$$

and $\sigma_{\alpha\beta}$ component of the conductivity tensor is:

$$\sigma_{\alpha\beta} = \frac{(-2e^2)}{(2\pi)^3} \int_{BZ} v_\alpha v_\beta \tau(\mathbf{k}) \frac{\partial f_0}{\partial E} d^3k. \tag{3.13}$$

If the metal is isotropic, its dispersion law in the conduction band being $E(\mathbf{k}) = E_c + \frac{\hbar^2 k^2}{2m_n}$ with an isotropic effective mass m_n, after transforming $\mathbf{k}$-integral to an integral over the energy in the conduction band, one obtains:

$$\sigma = \frac{ne^2 \langle \tau \rangle}{m_n}, \tag{3.14}$$

with n being the free carriers density in the conduction band and:

$$\langle \tau \rangle = \frac{\int_0^\infty \left(-\frac{\partial f_0}{\partial E} \right) \tau(E) E^{3/2} dE}{\int_0^\infty \left(-\frac{\partial f_0}{\partial E} \right) E^{3/2} dE}. \tag{3.15}$$

At intermediate temperatures, around Debye's temperature T_D (the temperature associated to the highest energy of acoustic phonon modes, $k_B T_D = \hbar \omega_{ac,max}$), the main scattering mechanism in metals is associated to electron-acoustic phonon interaction. In this case the relaxation time depends on the electron energy as in:

$$\tau(E) = cE^{3/2} \frac{T_D^5}{T^5 D_5 \left(\frac{T_D}{T} \right)}, \tag{3.16}$$

where c is a constant and

$$D_5 \left(\frac{T_D}{T} \right) = \int_0^{\frac{T_D}{T}} \frac{x^5 e^x}{(e^x - 1)^2} dx \tag{3.17}$$

is order-5 Debye's integral. Taking into account that for a metal $-\frac{\partial f_0}{\partial E} = \delta(E - E_F)$, where $\delta(x)$ is Dirac's function, eqs. (3.14,3.15) lead to:

$$\sigma = \frac{ne^2 c E_F^{3/2}}{m_n} \frac{T_D^5}{T^5 D_5 \left(\frac{T_D}{T} \right)}, \tag{3.18}$$

or

$$\rho = \frac{1}{\sigma} = 4\rho_0 \frac{T^5}{T_D^5} D_5 \left(\frac{T_D}{T} \right), \tag{3.19}$$

where ρ is the resistivity and $\rho_0 = \frac{m_n}{4ne^2 c E_F^{3/2}}$.
Eq. (3.19) has two important asymptotic forms.

Low temperatures, i.e. $T \ll T_D$
In this case $D_5 \left(\frac{T_D}{T} \right) \approx D_5(\infty) = \int_0^\infty \frac{x^5 e^x}{(e^x - 1)^2} dx = b$ (a constant value). Consequently:

$$\rho = 4\rho_0 b \frac{T^5}{T_D^5}, \tag{3.20}$$

which is the so-called "T^5 law", typical for simple metals at low temperatures.

High temperatures, i.e. $T \gg T_D$
In this case $\frac{T_D}{T} \ll 1$ and by considering Taylor series to third order in the denominator of the integrand in Debye's integral, one obtains:

$$\frac{x^5}{(e^x-1)(1-e^{-x})} \approx \frac{x^5}{(1+x+\frac{x^2}{2}+\frac{x^3}{6}-1)(1-1+x-\frac{x^2}{2})+\frac{x^3}{6}} \approx \frac{x^3}{1+\frac{x^2}{12}} \approx x^3\left(1-\frac{x^2}{12}\right) \tag{3.21}$$

and the resistivity (3.19) is given by

$$\rho(T) = \rho_0 \frac{T}{T_D}\left[1-\frac{1}{18}\left(\frac{T_D}{T}\right)^2\right]. \tag{3.22}$$

The last equation may be used to experimentally determine ρ_0 and T_D from the temperature dependence of the reistivity: plotting $\frac{\rho}{T} = f\left(\frac{1}{T^2}\right)$ one obtains a straight line with the slope $-\frac{\rho_0 T_D}{18}$ and the intercept on y-axis $\frac{\rho_0}{T_D}$.

If the temperature is much higher than T_D, eq. (3.22) simplifies to:

$$\rho = \rho_0 \frac{T}{T_D}, \tag{3.23}$$

and the resistivity changes linearly with T.

3.2 Experimental setup and procedure

The experimental setup is shown in Fig.3.1. The sample is a copper wire (10 m length, 0.1 mm diameter) wrapped around a glass rod introduced in an oven. The temperature of the wire is monitored by using a thermocouple. In the temperature range covered in this experiment the thermocouple sensitivity is constant, with a value of 24.6 K/mV.
Rise steadily the temperature inside the oven, starting from room temperature to a maximum of 200°C and measure the corresponding variation of the electrical resistance of the copper sample by using a multimeter.

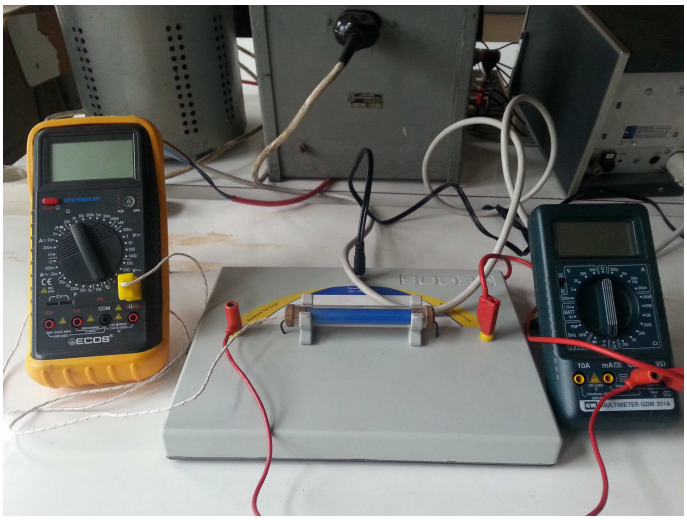

Fig. 3.1. Experimental setup for measurements of the temperature dependence of the electrical resistivity of metals.

3.3 Tasks

- Plot the temperature dependence of the resistance and compare it to theoretical predictions (3.23,3.22). Explain the experimental results. Since the resistance is given by the well-known expression $R = \rho\frac{l}{S}$, l being the length and S the transverse area of the sample, what about the effect of the temperature on the geometrical factor $\frac{l}{S}$?
- Copper crystallizes in a face-centered-cubic (fcc) form, the lattice constant being $a = 3.6\,\mathring{A}$. It is a monovalent chemical element with electron configuration $[\mathrm{Ar}]3d^{10}4s^1$ and the states in the lower part of the conduction band originate essentially from atomic $4s$ levels. Based on these informations, evaluate the density of electrons in the conduction band of copper. Using eq. (3.14), evaluate and plot the temperature dependence of the relaxation time $\langle\tau\rangle$. Use the value $m_n \approx 9.1 \times 10^{-31}$ kg for the effective mass.

4

Determination of the band-gap of germanium from electrical measurements

4.1 Theory

Suppose we are dealing initialy with some crystal consisting of $N = N_1N_2N_3$ primitive cells, $N_i,\ i = 1, 2, 3$ being the numbers of primitive cells following the directions of fundamental vectors of its crystalline lattice $\{\mathbf{a}_1, \mathbf{a}_2, \mathbf{a}_3\}$. Its size in $\mathbf{a}_i$ direction is then $L_i = N_i a_i$, N_i being a *macroscopically large number*. Since in this case most of the atoms of the crystal are in its volume rather that on the surface, the "volume" properties dominates. We will eliminate the surface by identically repeating the initial crystal over directions of $\mathbf{a}_1, \mathbf{a}_2, \mathbf{a}_3$ vectors, until all the physical space is filled. [1]
With this model of a crystalline solid, due to its translational invariance (which is the fundamental symmetry of the crystalline lattice), all one-particle wave functions must have the following analytical structure:

$$\psi_{n\mathbf{k}\sigma}(\mathbf{r}) = u_{n\mathbf{k}\sigma}(\mathbf{r})e^{i\mathbf{k}\cdot\mathbf{r}} \tag{4.1}$$

$$u_{n\mathbf{k}\sigma}(\mathbf{r}) = u_{n\mathbf{k}\sigma}(\mathbf{r} + \mathbf{R}), \tag{4.2}$$

for each Bravais vector $\mathbf{R} = n_1\mathbf{a}_1 + n_2\mathbf{a}_2 + n_3\mathbf{a}_3$. The quantum numbers $n, \mathbf{k}, \sigma$ represent, respectively:
- n: band index;
- $\mathbf{k}$: the wave vector;
- σ: spin projection.

Wave functions of the form (4.1) are called *Bloch's functions*; in a perfect crystal all one-particle wave functions must be then Bloch' functions; a typical form is shown in Fig. 4.1.

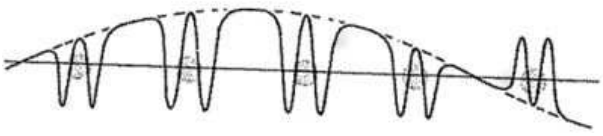

Fig. 4.1. The real part of a typical Bloch function in one dimension. The dotted line corresponds to $e^{i\mathbf{k}\cdot\mathbf{r}}$ factor and light circles represent atoms. (from `en.wikipedia.org/wiki/Bloch_wave`)

They obey periodic boundary conditions (or Born - von Karmann boundary conditions):

$$\psi_{n\mathbf{k}\sigma}(\mathbf{r}) = \psi_{n\mathbf{k}\sigma}(\mathbf{r} + N_1\mathbf{a}_1) = \psi_{n\mathbf{k}\sigma}(\mathbf{r} + N_2\mathbf{a}_2) = \psi_{n\mathbf{k}\sigma}(\mathbf{r} + N_3\mathbf{a}_3), \tag{4.3}$$

[1] This model works as long as the initial assumption on the number of atoms on the surface being negligibly small as compared with the number of atoms in the volume is true. It will not be satisfactory in the case of, e.g. very thin films, or very small systems with sizes of tens to a few hundreds of lattice constants.

which define the allowed values for $\mathbf{k}$:

$$k_i = \frac{2\pi}{N_i a_i} n_i,\ n_i \in \left[-\frac{N_i}{2}, \frac{N_i}{2} \right) \tag{4.4}$$

lying in a Wigner-Seitz cell in the reciprocal space called the first Brillouin's zone, $k_i = \mathbf{k} \cdot \frac{\mathbf{a}_i}{a_i}$ being the projection of $\mathbf{k}$ on the direction of $\mathbf{a}_i$. Note that there are N allowed values for $\mathbf{k}$, very densely distributed: two allowed values for k_i are separated by $\Delta k_i = \frac{2\pi}{N_i a_i}$ which is a small value. Introducing the fundamental vectors $\{\mathbf{b}_1, \mathbf{b}_2, \mathbf{b}_3\}$ of the reciprocal lattice associated to the crystalline lattice and taking into account that $\mathbf{a}_i \cdot \mathbf{b}_j = 2\pi\delta_{ij}$ (δ_{ij} being Kronecker's symbol), one writes

$$\mathbf{k} = \frac{n_1}{N_1}\mathbf{b}_1 + \frac{n_2}{N_2}\mathbf{b}_2 + \frac{n_3}{N_3}\mathbf{b}_3,\ n_i \in \left[-\frac{N_i}{2}, \frac{N_i}{2} \right) . \tag{4.5}$$

To each Bloch' state (4.1) will correspond an energy level $E_{n\sigma}(k)$. For each n value there are N very densely distributed levels, corresponding to the above mentioned $\mathbf{k}$ values, forming a band of allowed energies.
Consequently, the energy spectrum of electrons in perfect crystalline solids consists of bands of allowed energies separated by forbidden gaps where there are no energy levels at all. If there are s atoms in the primitive cell (forming the base of the crystal) each with g_s orbital degeneracy, the allowed bands will consist of $s \cdot g_s$ branches with N $\mathbf{k}$-values each, so $g_s s N$ energy levels.

Suppose there are N_e electrons in the considered crystal. Electrons are fermions, so each allowed state will be occupied following Pauli's exclusion principle. Two kinds of ground (or fundamental) states will arise:

- after occuping each allowed state characterized by a $n, \mathbf{k}, \sigma$ set with electrons, the states of a number of energy bands will be completely occupied, while the bands lying above in energy will be completely empty; such a crystal is called a dielectric (or insulator), because in its fundamental state, at absolute zero temperature, its electrons do not flow freely under the influence of a small electric field (because there are no available states to be excited into by the small electric field). The electrical conductivity of insulators is zero in their ground state. Occupied bands are called valence bands. The first (completely) unoccupied band is called conduction band. The energy separation between the last valence band and the conduction band is called the band-gap. If the band-gap is less than 3 eV, the material is called a semiconductor. The reason for this is that at non-zero temperatures in such materials a number of electrons will be thermally excited from the last valence band into states in the conduction band; two kinds of excitations are created following this process: the *conduction electron*, occupying states in the conduction band, and the *hole* occupying states in the valence band. Both conduction electrons and holes (corresponding to a broken chemical bond in the crystal) can move freely, as they now occupy Bloch's states in incompletely filled bands, with a large density of states freely available at close energies.

- after occuping each allowed state characterized by a $n, \mathbf{k}, \sigma$ set with electrons, the states of a number of energy bands will be completely occupied, while the last band with occupied states is only partialy filled; such a crystal is called a metal (or conductor). The last partially filled band is called conduction band. The last occupied level in the conduction band in the ground state is called *Fermi level*. The set of states at Fermi energy is called *Fermi sea*. The electrons occupying extended Bloch's states at Fermi sea can be easily accelerated by a small electric field, as there are many free states available at close energies; so the electrical conductivity of a metal is non-zero in its ground state.

Real crystals are not perfect. There are always some defects, some point-like (impurities, vacancies, interstitials) other extended (dislocations, grain boundaries, surface). All these defects will break the translational symmetry of a perfect crystal. If they do not alter significantly the crystalline order (in other words, if the disorder degree is small), the potential energy describing their interaction with the electrons of the host crystal will act as a small localized (in space and time) perturbation to the one-particle Hamiltonian corresponding to the perfect crystal. Consequently, when analyzing the dynamics of free charge carriers (electrons in the

conduction band of metals or conduction electrons and holes in semiconductors), those defects will scatter the carriers from one Bloch's state to another in the same band. Due to these frequent scattering events, the momentum and/or the energy of the carriers will relax (free carriers cannot be continuously accelerated by an electric field, they will loose momentum and/or energy due to scattering by defects), which implies that the electrical conductivity is *finite* and the current density **j** obeys Ohm's law:

$$\mathbf{j} = \hat{\sigma} \cdot \mathbf{E}, \tag{4.6}$$

E being the applied electric field and $\hat{\sigma}$ the 2-order conductivity tensor.

Even if the crystals were perfect, there is a source of crystalline disorder at non-zero temperature: the atomic nuclei the crystal consists of vibrate around their equilibrium positions at T = 0 K. The vibrational state may be described in terms of normal modes. A normal vibration mode of a crystal is called a *phonon*. If there are s atoms in the primitive cell, there will be $3s$ phonon branches, each with N phonon modes. There are essentially two types of phonons: acoustic phonons (all the atoms in the primitive cell oscillate in phase) and optical (the atoms in the primitive cell oscillate out-of-phase). Since optical phonons tend to change the length of chemical bonds, they require more energy as compared to acoustic ones. By breaking the translational symmetry, phonons will scatter free carriers.

Resuming, we can classify the scatterers as:
- static: they only scatter free carriers elastically (the momentum of free carriers is relaxed, their energy being conserved; examples: point-like or extended defects with no internal degrees of freedom);
- dynamic: they scatter free carriers inelastically (both the energy and momentum are relaxed; example: electron-phonon interaction, electron-electron interaction, impurities with internal degrees of freedom accessible at typical energies of free carriers).

Taking into account the interaction free carrier - scatterer, the electrical conductivity of a crystal can be determined, e.g. in the frame of Boltzmann's approach in the relaxation time approximation. For an isotropic semiconductor, it is given by:

$$\sigma = e\mu_n n + p\mu_p p \tag{4.7}$$

where n, p are respectively electrons and holes densities, e is the electron charge and μ_n, μ_p are electrons and holes mobilities, given by

$$\mu_{n,p} = \frac{e\langle\tau_{n.p}\rangle}{m_{n,p}}. \tag{4.8}$$

In the above equation $m_{n,p}$ is the effective mass of free carriers in the conduction and respectively valence band and $\langle\tau_{n.p}\rangle$ is the relaxation time for electrons and holes, respectively (the mean time between collisions of free carriers by static and/or dynamic scatterers). For a non-degenerate semiconductor $n = N_c \exp\left(\frac{E_F - E_c}{k_B T}\right)$, $n = N_v \exp\left(\frac{E_v - E_F}{k_B T}\right)$, $N_{c,v}$ being the effective density of states in the conduction and, respectively, valence band, E_v is the superior limit of the valence band, E_c is the inferior limit of the conduction band, E_F is the Fermi level located in this case in the forbidden gap, k_B is Boltzmann's constant and T is absolute temperature.

The conductivity of semiconductors varies with temperature (Fig. 4.2). Three ranges can be identified:

- At low temperatures extrinsic conduction dominates (range I). As the temperature rises, charge carriers are activated from the electrically active impurities (donors or acceptors). As a consequence, the activation energy of the free carriers density and of the conductivity is given by the ionization energy of donors or acceptors.
- At moderate temperatures, when all electrically active impurities are ionized (range II), the impurity depletion regime shows up, characterized by constant free carriers densities.

- At high temperatures (range III), intrinsic conduction regime dominates. Charge carriers are thermally excited from the valence band to the conduction band, their densities being much larger than the densities of impurity centers. The temperature dependence is in this case essentially described by an exponential function.

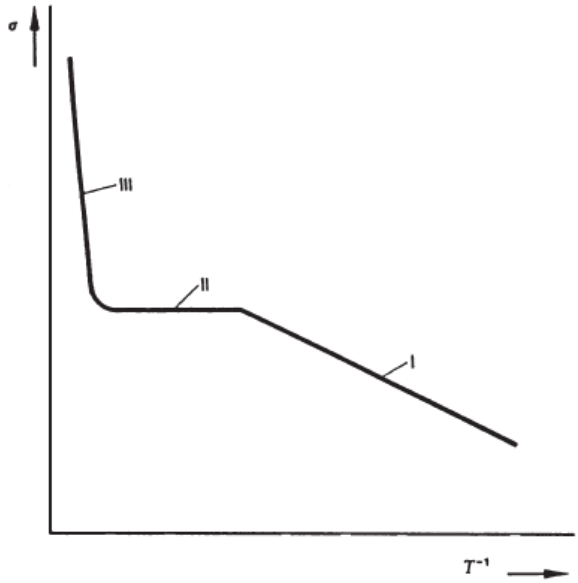

Fig. 4.2. Conductivity of a semiconductor as a function of the reciprocal of the temperature.

In the intrinsic conduction regime (range III, Fig. 4.2), $n = p = n_i$, with the intrinsic free carriers density:

$$n_i = \sqrt{N_c N_v}\, e^{-\frac{E_g}{2k_B T}} \tag{4.9}$$

$E_g = E_c - E_v$ being the band-gap. Note that $N_{c,v} \propto T^{3/2}$ and the temperature dependence of the relaxation times is given by a power-law for the most important scatterers $\langle \tau_{n.p} \rangle = CT^r$, C being a constant (independent of T).
Collecting all the above results, it follows that the temperature dependence of the conductivity of an intrinsic semiconductor is given by

$$\sigma = e(\mu_n + \mu_p) n_i = AT^s \exp\left(-\frac{E_g}{2k_B T}\right), \tag{4.10}$$

with $s = r + \frac{3}{2}$.
By experimentally measuring the conductivity at different temperatures and plotting $\ln \sigma \cdot T^{-s} = f\left(\frac{10^3}{T}\right)$ one will obtain a straight line with the slope $-\frac{E_g}{2k_B \cdot 10^3}$, from which the band-gap E_g can be extracted.

4.2 Experimental setup and procedure

The experimental setup is shown in Fig.4.3. The module with a monocrystalline germanium test sample is directly connected with the 12 V output of the power unit over the ac-input on the back-side of the module. The voltage across the sample is measured with a multimeter connected to the two sockets in the lower part on the front-side of the board. The current and temperature values can be easily read on the integrated display

Table 4.1. Values of exponents r and s characterizing temperature dependences of free carriers mobilities and of the conductivity of semiconductors, for the most important scattering mechanisms. T_D is Debye's temperature.

Scatterer	r	s
neutral impurity	0	$\frac{3}{2}$
ionized impurity	$\frac{3}{2}$	3
acoustic phonons	$-\frac{1}{2}$	1
optical phonons ($T > T_D$)	$\frac{1}{2}$	2

of the module. Be sure, that the display works in the temperature mode during the measurement. You can change the mode with the "Display"-knob.

Fig. 4.3. Experimental setup for the determination of the band-gap of germanium.

Set the current to a value of 5 mA. The current source will maintain the current nearly constant during the measurement, but the voltage will change with the temperature.

Set the display in the temperature mode. Start the software for measurement configuration and data acquisition and choose Cobra3 as gauge. You will receive first the configuration screen shown in Fig. 4.4. Choose parameters that have to be measured and displayed, e.g. the voltage across the sample as a function of temperature. Select all other parameters as shown in Fig. 4.4. Press the "Continue" button. Start the measurement by activating the heating coil with the "ON/OFF"-knob on the backside of the module and starting the software.

Record the voltage across the sample as a function on temperature, for a temperature range from room temperature to a maximum of 170°C. You will receive a typical curve as shown in Fig.4.5.

4.3 Tasks

Since germanium is a cubic semiconductor, its conductivity is given by:

$$\sigma = \frac{1}{\rho} = \frac{l}{S}\frac{I}{U}, \tag{4.11}$$

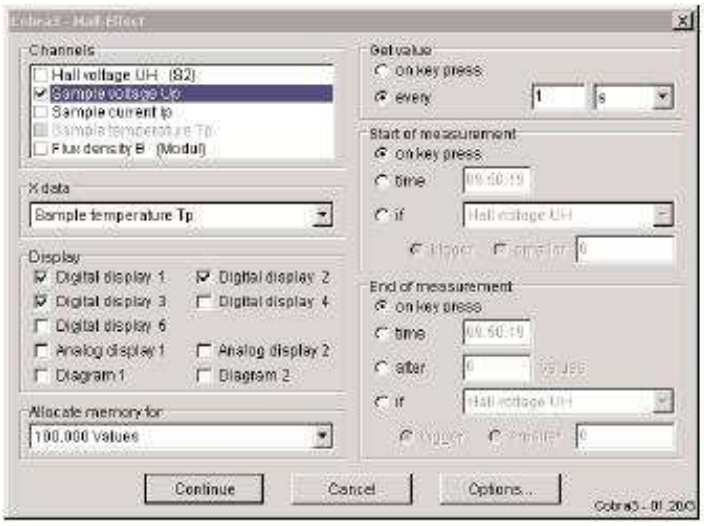

Fig. 4.4. Start menu of the Cobra3 software for measurement configuration and data acquisition.

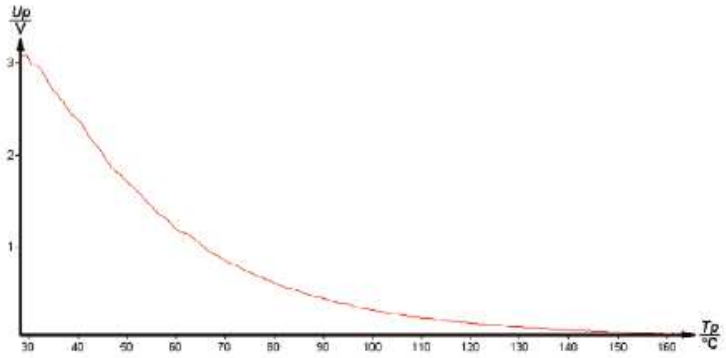

Fig. 4.5. Typical experimental results of the voltage measurement as a function of temperature.

where S is the cross-section area of the sample and l its length. The size of the sample is $20 \times 10 \times 1\,\mathrm{mm}^3$.

- With the measured values, plot $\ln \sigma T^{-s} = f\left(\frac{10^3}{T}\right)$, by choosing from Table 4.1 the value of the exponent s associated to the scattering mechanism you consider to be dominant in this case. Argue your choice.
- By performing a linear regression of the experimental curve with the expression (see eq.(4.10))

$$\ln \sigma \cdot T^{-s} = \ln A - \frac{E_g}{2k_B \cdot 10^3} \frac{10^3}{T} \tag{4.12}$$

calculate from the slope the band-gap E_g of germanium. Boltzmann's constant is $k_B = 8.625 \times 10^{-5}$ eV/K.

5

Hopping conduction in semiconductors

5.1 Theory

In a perfect semiconducting crystal the ground state at $T = 0\,K$ correspond to completely filled valence bands, while de band higher in energy than the last valence band (the conduction band) is completely empty. All states in allowed energy bands in the energetic spectrum are extended Bloch states.
For technological applications, semiconductors are doped: impurities are introduced in the crystalline structure in a controlled way. Electronic states associated to those impurities are of a very different nature as compared with the host Bloch state: they are *localized* (Fig. 5.1b). This is due to the fact that impurity centers are located randomly in the host crystal, so the translational symmetry, which is the origin of the extended character of Bloch host states, is broken. In other words, a degree of *disorder* has been introduced in the system. Of practical importance are impurity centers with energy levels in the bandgap, which may act as donors if the corresponding energy level E_D is close to the conduction band (shallow donor, $E_c - E_D \approx k_B T$), as acceptors if the corresponding energy level E_A is close to the valence band (shallow acceptor, $E_A - E_v \approx k_B T$), or as trapping/recombination centers if the corresponding level is deep in the bandgap ($|E_t - E_{c,v}| \gg k_B T$) (Fig. 5.1a). Shallow impurities paly an important role in semiconductor physics: a shallow donor is easily ionized by transfering an electron on an extended state in the conduction band, while a shallow acceptor will capture an electron from the valence band, this way creating a hole in the valence band.

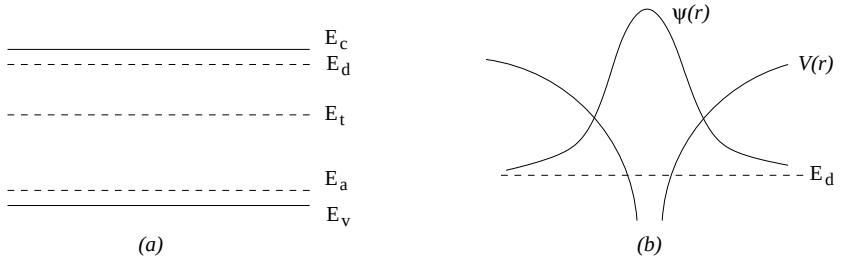

Fig. 5.1. (a) Impurity levels in the bandgap of a semiconductor: donor, acceptor and trappinng levels; (b) schematics of a localized state and potential energy well associated to a donor impurity.

Localized states in crystals are always associated with disorder. The higher the disorder degree, the higher the density of localized states. Crystalline disorder is not exclusively associated with impurities: structural defects of any kind (point-defects like vacancies or interstitials, one-dimensional extended defects like dislocations or two-dimensional extended defects like surface or grain boundaries) will also break tranlational symmetry, leading to localized state. An extreme case is that of amorphous materials, where the long range order is completely lost.

Both theory and experiment show that with increasing disorder band tails appear, with energy levels associated to localized states, while the states with energy levels in the middle of the band remain extended (Fig. 5.2).

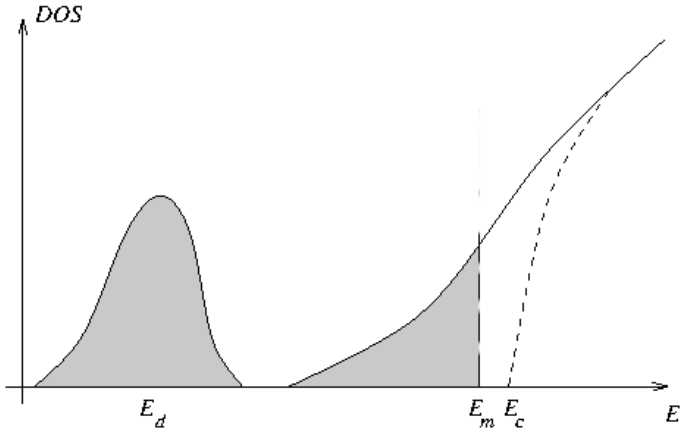

Fig. 5.2. Schematics of density of states (DOS) near conduction band in a disordered semiconductor. Shaded areas correspond to localized states. E_d is a donor impurity band and E_m is the energy level in the conduction band separating band tail localized states from extended states. DOS in a perfect crystal is drawn with dotted line.

Due to the presence of localized states, a new type of conduction mechanism may show-up in disordered semiconductors: at low enough temperatures the main contribution to charge transport comes from electrons hopping directly between localized states (Fig. 5.3), without reaching extended states in the conduction (or valence) band. This is called *hopping transport*. Electrons jump from occupied impurity centers to empty ones, so empty impurity centers have to exist to make the hopping conduction possible. This comes from partial compensation, e.g. of donor centers by some acceptor centers with much lower density.

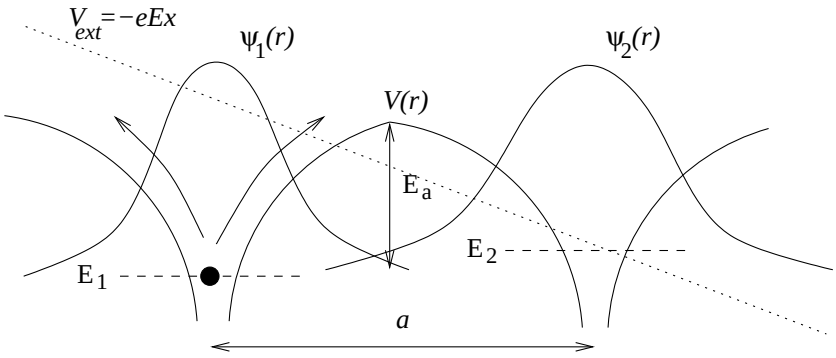

Fig. 5.3. (a) Impurity levels in the bandgap of a semiconductor: donor, acceptor and trappinng levels; (b) schematics of a localized state and potential energy well associated to a donor impurity.

The hopping transport mechanism leads to a very low mobility of charge carriers, since the electron jumps are associated with a weak overlap of the localized states centered on first-neighbour donors. It wins in the competition with the band conduction mechanism, involving extended states and high electron mobilities, only because if the temperature is low enough the denisty of electrons occupying extended band states is exponentially small. It follows that hopping conduction is favoured by:
- low temperatures;

- high densities of impurity centers;
- high values of the bandgap.

Let's begin by considering a simple model for the hopping conductivity: the electron is localized on a impurity center in a potential well with an energy barrier E_a (Fig. 5.3). Jumps to nearby empty centers can be described as a tunneling process assisted by phonons. Optical phonons are involved in this process, because in the case of optical modes the distance between centers varies as they oscillate out-of-phase, and so the overlap of the wave-functions varies also, increasing or decreasing the jump probability. In thermal equilibrium, the jump frequency (jump probability per second) is the same, in average, in all directions, consequently there is no net flow of charges. The jump frequency is given by:

$$\nu = \nu_{ph} \exp\left(-\frac{E_a}{k_B T}\right), \tag{5.1}$$

where ν_{ph} is the typical phonon frequency, E_a is the barrier height, k_B is Boltzmann's constant and T is absolute temperature. If a stationary electrical field is applied electron jumps will be oriented in average along the direction of the field. This is due to the fact that the barrier height is reduced in the direction of the field (see figure 5.3, where the barrier is reduced to $E_a - \frac{1}{2}eEa$ towards the anode and is increased to $E_a + \frac{1}{2}eEa$ towards the cathode). The average jump frequency in the field direction is given by:

$$\Delta\nu_E = \nu_{ph} \exp\left(-\frac{E_a - \frac{1}{2}eEa}{k_B T}\right) - \nu_{ph} \exp\left(-\frac{E_a + \frac{1}{2}eEa}{k_B T}\right) = 2\nu_{ph} \exp\left(-\frac{E_a}{k_B T}\right) \sinh\left(\frac{eEa}{2k_B T}\right), \tag{5.2}$$

which, for low field values $eEa \ll k_B T$, becomes:

$$\Delta\nu_E = \frac{e\nu_{ph} Ea}{k_B T} \exp\left(-\frac{E_a}{k_B T}\right), \tag{5.3}$$

a being the average separation distance between impurity centers.

If the density of electrons able to jump is n, then the current density can be evaluated as $j = en\overline{v} = ena\Delta\nu_E$ which, with eq. (5.3), reads:

$$j = \frac{e^2 n\nu_{ph} Ea^2}{k_B T} \exp\left(-\frac{E_a}{k_B T}\right). \tag{5.4}$$

Eq. (5.4) is Ohm's law in local form, $j = \sigma E$, with the hopping conductivity:

$$\sigma_h = \frac{e^2 n\nu_{ph} a^2}{k_B T} \exp\left(-\frac{E_a}{k_B T}\right). \tag{5.5}$$

Consequently, the hopping mobility is:

$$\mu_h = \frac{e\nu_{ph} a^2}{k_B T} \exp\left(-\frac{E_a}{k_B T}\right), \tag{5.6}$$

and its temperature dependence is of activated type. This exponential temperature dependence of the mobility is a signature for hopping conduction. In the case of band conduction mechanism, the temperature dependence of the mobility reflects the dominant scattering mechanism and is at most a power function.

A more realistic model for hopping transport, based on percolation theory, gives the same temperature dependence for the hopping conductivity and mobility, with a refined activation energy E_a, related to the amplitude of characteristic fluctuations of potential energy due to disorder. In addition, considering the resistivity

$$\rho_h = \rho_{0h} \exp\left(\frac{E_a}{k_B T}\right) \tag{5.7}$$

the pre-exponential factor ρ_{0h} depends exponentially on the density of impurity centers N_i:

$$\rho_{0h} = \rho_0 e^{f(N_i)}. \tag{5.8}$$

The physical reason for the dependence (5.8) is as follows: the jump probability is determined by the wave-function overlap. Since the separation between impurity or defect centers is usually larger than the localization radius (at a moderate disorder degree), the overlap integrals drop exponentially with the distance between centers. This exponential dependence is considered to be the main experimental evidence for the hopping transport mechanism.

5.2 Experimental setup and procedure

The experimental setup is shown in Fig.5.4. The sample is a piece of ceramic (an alloy of manganese, cobalt and bismuth oxides), introduced in an electrical oven. The temperature of the sample is monitored by using a thermocouple. In the temperature range covered in this experiment the thermocouple sensitivity is constant, with a value of 24.6 K/mV.
Rise steadily the temperature inside the oven, starting from room temperature to a maximum of 100°C and measure the corresponding variation of the electrical resistance of the sample by using a multimeter. Begin by setting the value of the heating current to 0.8 A and then increase it in steps of 0.5 A if the temperature stops to increase. Do NOT use a heating current more than 2.5 A!

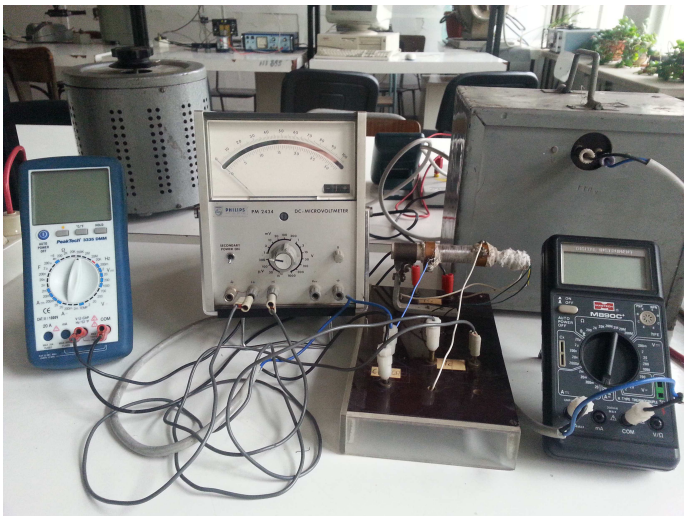

Fig. 5.4. Experimental setup for measurements of the temperature dependence of the hopping resistivity.

5.3 Tasks

- With the geometric shape of the sample, $R\,[k\Omega] = 0.25 \times \rho\,[k\Omega \cdot m]$. Plot the temperature dependence of the resistivity and compare it to theoretical predictions (5.7). You will use an Arrhenius plot to show your data: $\ln \rho = f\left(\frac{10^3}{T}\right)$. Evaluate the activation energy E_a.
- Evaluate the phonon frequency ν_{ph}, knowing that $k_B = 8.625 \times 10^{-5}$ eV/K, $a = 8.27$ $\mathring{A}$ and $n = 3.6 \times 10^{18}$ cm^{-3}.

6

Hall effect in semiconductors

6.1 Theory

The Hall effect is the production of a voltage drop (the Hall voltage) across an electrical conductor placed in a magnetic field perpendicular to an electric current in the conductor. The Hall voltage is measured along the direction which is perpendicular to the plane defined by the current density **j** and the magnetic field **B** (Fig. 6.1). It is due to Lorentz's force acting on free carriers moving in a transverse magnetic field and diverging them towards a lateral surface on y direction, until the electric field developing on y is intense enough to compensate Lorentz's force:

$$\mathbf{F}_H = -\mathbf{F}_L, \tag{6.1}$$

where $\mathbf{F}_H = q\mathbf{E}_H$ and $\mathbf{F}_L = q\mathbf{v} \times \mathbf{B}$, q is the charge of majority carriers, $\mathbf{E}_H$ is the Hall field. The sign of the Hall field indicates the conduction type of the analyzed sample; it follows that the Hall effect can be used to identify the conduction type of semiconductors.

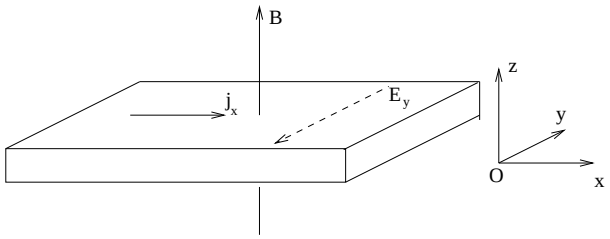

Fig. 6.1. Hall effect on a rectangular n-type semiconductor sample.

The Hall field $E_y = E_H$ is proportional to the current density j_x and the magnetic field B, if the magnetic field is not too high ($\mu_n B < 1$, μ_n being the mobility of majority charge carriers, supposed here to be electrons). Quantitatively, the Hall effect is described by the Hall constant, defined as follows:

$$R_H = \frac{E_H}{j_x B}. \tag{6.2}$$

The Hall constant is related to the electronic properties of the (semi)conductor material. In the frame of Boltzmann's approach to the transport phenomena in solids, electrical conductivity in a transverse magnetic field becomes a 2-order tensor even in the case of isotropic (cubic) materials, due to the anisotropy introduced by the magnetic field $\mathbf{B} = (0, 0, B)$ (see subsection 6.1.1 for details):

$$\hat{\sigma} = \begin{pmatrix} \sigma_{xx} & \sigma_{xy} & 0 \\ -\sigma_{xy} & \sigma_{xx} & 0 \\ 0 & 0 & \sigma_{zz} \end{pmatrix} \tag{6.3}$$

where

$$\sigma_{xx} = \frac{ne^2}{m^*} \left\langle \frac{\tau(\mathbf{k})}{1+\omega_c^2\tau^2(\mathbf{k})} \right\rangle \tag{6.4}$$

$$\sigma_{xy} = -\frac{ne^2}{m^*} \left\langle \frac{\omega_c\tau^2(\mathbf{k})}{1+\omega_c^2\tau^2(\mathbf{k})} \right\rangle, \tag{6.5}$$

$\omega_c = \frac{eB}{m^*}$ being the cyclotron pulsation for the carriers with effective mass m^*, e being the absolute value of electron charge and n the majority carriers density. The mean value $\langle\tau\rangle$ is given by:

$$\langle\tau\rangle = \frac{\int_0^\infty \left(-\frac{df_0}{dE}\right)\tau(E)E^{3/2}dE}{\int_0^\infty \left(-\frac{df_0}{dE}\right)E^{3/2}dE}, \tag{6.6}$$

where $f_0(E)$ is Fermi-Dirac distribution function, E is the energy of the carrier in the band and $\tau(E)$ is the relaxation time of the momentum and/or energy due to scattering of charge carriers by defects.

Ohm's law, $\mathbf{j} = \hat{\sigma}\cdot\mathbf{E}$, in the experimental conditions corresponding to the Hall effect measurements (i.e. $j_y = 0$), leads to:

$$j_x = \sigma_{xx}E_x + \sigma_{xy}E_y \tag{6.7}$$

$$0 = -\sigma_{xy}E_x + \sigma_{xx}E_y. \tag{6.8}$$

From eqs. (6.2,6.7,6.8) one obtains:

$$R_H = \frac{1}{B}\frac{\sigma_{xy}(B)}{\sigma_{xx}^2(B)+\sigma_{xy}^2(B)}, \tag{6.9}$$

which for not too high magnetic fields (i.e. $\omega_c\tau = \mu B < 1$) and supposing that majority carriers are electrons with density n simplifies to:

$$R_H = -\frac{1}{ne}\frac{\langle\tau^2\rangle}{\langle\tau\rangle^2}. \tag{6.10}$$

If majority carriers are holes in the valence band of a semiconductor, with density p, the expression for the Hall constant reads:

$$R_H = \frac{1}{pe}\frac{\langle\tau^2\rangle}{\langle\tau\rangle^2}. \tag{6.11}$$

The ratio $r_H = \frac{\langle\tau^2\rangle}{\langle\tau\rangle^2}$ is called Hall scattering factor; it depends on the main scattering mechanism controlling the scattering of majority charge carriers in the sample. Its values for the most important scatterers are collected in table 6.1.

Suppose the analyzed semiconductor sample is n-type (majority carriers are conduction band electrons). If the longitudinal conductivity of the sample is measured independently in the absence of magnetic field, since $\sigma = ne\mu_n$, one obtains:

$$|R_H|\sigma = \mu_n r_H = \mu_H, \tag{6.12}$$

which is called Hall mobility.

Table 6.1. Values of the Hall scattering factor in semiconductors, for the most important scattering mechanisms. T_D is Debye's temperature.

Scatterer	r_H
neutral impurity	1
ionized impurity	$\frac{315\pi}{512}$
acoustic phonons	$\frac{3\pi}{8}$
optical phonons ($T << T_D$)	1
optical phonons ($T > T_D$)	$\frac{45\pi}{128}$

It follows that the temperature dependent Hall effect can be used for a complete characterization of the electronic properties of semiconductors, since it gives:
- the conduction type of the sample;
- the temperature dependence of the majority carriers density $n(T)$, from which the bandgap E_g and the ionization energy of the main donor can be extracted;
- the temperature dependence of the Hall mobility $\mu_H(T)$, from which informations about the scattering mechanisms can be extracted.
The Hall effect is of utmost importance in the solid state physics.

6.1.1 Boltzmann's equation

We are interested in describing the charge transport in magnetic fields in the case of a semiconductor sample. For the sake of simplicity, we will consider the case of an isotropic crystal: a cubic semiconductor, let's say with a n-type conduction ($n \gg p$, n is the density of electrons in the conduction band, p is the density of holes in the valence band). Then the dispersion relation for the conduction band reads:

$$\mathcal{E}(\mathbf{k}) = \mathcal{E}_c + \frac{\hbar^2 k^2}{2m_n}, \tag{6.13}$$

with m_n the isotropic effective mass. The average velocity of electrons in a Bloch state is then:

$$\mathbf{v} = \frac{1}{\hbar}\nabla_{\mathbf{k}}\mathcal{E}(\mathbf{k}) = \frac{\hbar\mathbf{k}}{m_n}. \tag{6.14}$$

Let $\mathbf{E}$, $\mathbf{B}$ be the externally applied electric and magnetic fields. We only consider here the case of *stationary and uniform* fields.

Recall that Boltzmann's equation for the one-particle distribution function $f(\mathbf{r}, \mathbf{k}, t)$ reads:

$$\frac{\partial f}{\partial t} + \mathbf{v}\cdot\nabla_{\mathbf{r}} f - \frac{e}{\hbar}(\mathbf{E} + \mathbf{v}\times\mathbf{B})\cdot\nabla_{\mathbf{k}} f = \left(\frac{\partial f}{\partial t}\right)_{coll.} \tag{6.15}$$

where we have explicitely taken into account that the electron charge is $(-e)$; the right-hand-side term is the collision integral, describing the scattering of conduction band electrons by the structural defects, impurities, phonons or other electrons. In the *relaxation time approximation* one writes this term as in:

$$\left(\frac{\partial f}{\partial t}\right)_{coll.} = -\frac{f - f_0}{\tau(\mathbf{k})} \tag{6.16}$$

where $\tau(\mathbf{k})$ is the momentum/energy relaxation time, and

$$f_0(\mathcal{E}(\mathbf{k})) = \frac{1}{1 + \exp\left(\frac{\mathcal{E}(\mathbf{k}) - E_F}{k_B T}\right)} \tag{6.17}$$

is the equilibrium Fermi-Dirac distribution function, E_F being the Fermi level, k_B Boltzmann's constant and T absolute temperature. Then, in the relaxation time approximation, Boltzmann's equation (6.15) reads:

$$\frac{\partial f}{\partial t} + \mathbf{v} \cdot \nabla_{\mathbf{r}} f - \frac{e}{\hbar}(\mathbf{E} + \mathbf{v} \times \mathbf{B}) \cdot \nabla_{\mathbf{k}} f = -\frac{f - f_0}{\tau(\mathbf{k})}. \tag{6.18}$$

Since the applied fields are uniform and stationary and we are only interested to describe the stationary case, there is no reason for f to depend on time and position. Then $f = f(\mathbf{k})$ and eq. (6.18) simplifies to the form:

$$-\frac{e}{\hbar}(\mathbf{E} + \mathbf{v} \times \mathbf{B}) \cdot \nabla_{\mathbf{k}} f = -\frac{f - f_0}{\tau(\mathbf{k})}. \tag{6.19}$$

In the next section we will try to solve the above equation for f.

The one-electron distribution function in stationary and uniform electric and magnetic fields

We are interested in the linear response relative to the applied electric field, so we search for the solution of the Boltzmann's equation as $f = f_0 + f_1(\mathbf{k})$, with $f_1(\mathbf{k})$ linear in $\mathbf{E}$. We will only keep systematically the terms linear in $\mathbf{E}$. In terms of the correction f_1, eq. (6.19) reads:

$$-\frac{e}{\hbar}\mathbf{E} \cdot \nabla_{\mathbf{k}}(f_0 + f_1) - \frac{e}{\hbar}(\mathbf{v} \times \mathbf{B}) \cdot \nabla_{\mathbf{k}} f_0 - \frac{e}{\hbar}(\mathbf{v} \times \mathbf{B}) \cdot \nabla_{\mathbf{k}} f_1 = -\frac{f_1}{\tau(\mathbf{k})}. \tag{6.20}$$

Since f_1 is linear in $\mathbf{E}$ and we are only interested in the linear response in E, we will neglect f_1 in the first term (with the electric field $\mathbf{E}$) in the above equation:

$$-\frac{e}{\hbar}\mathbf{E} \cdot \nabla_{\mathbf{k}} f_0 - \frac{e}{\hbar}(\mathbf{v} \times \mathbf{B}) \cdot \nabla_{\mathbf{k}} f_0 - \frac{e}{\hbar}(\mathbf{v} \times \mathbf{B}) \cdot \nabla_{\mathbf{k}} f_1 = -\frac{f_1}{\tau(\mathbf{k})}. \tag{6.21}$$

For reasons that will become clear below, we will search the solution to eq. (6.21) in the form:

$$f_1(\mathbf{k}) = \frac{\hbar}{m_n}\left(-\frac{\partial f_0}{\partial \mathcal{E}}\right)\mathbf{k} \cdot \mathbf{Z}(\mathcal{E}(\mathbf{k})), \tag{6.22}$$

where $\mathbf{Z}(\mathcal{E}(\mathbf{k}))$ is the new unknown function, to be determined.
Let's consider separately the terms in eq. (6.21):

$$-\frac{e}{\hbar}\mathbf{E} \cdot \nabla_{\mathbf{k}} f_0 = -\frac{e}{\hbar}\mathbf{E} \cdot \hbar\mathbf{v}\frac{\partial f_0}{\partial \mathcal{E}} = -e\mathbf{E} \cdot \mathbf{v}\frac{\partial f_0}{\partial \mathcal{E}}; \tag{6.23}$$

$$-\frac{e}{\hbar}(\mathbf{v} \times \mathbf{B}) \cdot \nabla_{\mathbf{k}} f_0 = -\frac{e}{\hbar}(\mathbf{v} \times \mathbf{B}) \cdot (\hbar\mathbf{v})\frac{\partial f_0}{\partial \mathcal{E}} = 0, \tag{6.24}$$

since $\mathbf{v} \cdot (\mathbf{v} \times \mathbf{B}) = 0$;

- taking into account eq. (6.22), one writes:

$$
\begin{aligned}
-\frac{e}{\hbar}(\mathbf{v}\times\mathbf{B})\cdot\nabla_{\mathbf{k}}f_1 &= \frac{e}{m_n}(\mathbf{v}\times\mathbf{B})\cdot\nabla_{\mathbf{k}}\left(\frac{\partial f_0}{\partial\mathcal{E}}\mathbf{Z}\cdot\mathbf{k}\right)\\
&= \frac{e}{m_n}(\mathbf{v}\times\mathbf{B})\cdot\left(\frac{\partial f_0}{\partial\mathcal{E}}\nabla_{\mathbf{k}}(\mathbf{Z}\cdot\mathbf{k})+(\mathbf{Z}\cdot\mathbf{k})\frac{\partial^2 f_0}{\partial\mathcal{E}^2}\hbar\mathbf{v}\right)\\
&= \frac{e}{m_n}\frac{\partial f_0}{\partial\mathcal{E}}(\mathbf{v}\times\mathbf{B})\cdot\nabla_{\mathbf{k}}(\mathbf{Z}\cdot\mathbf{k})\\
&= \frac{e}{m_n}\frac{\partial f_0}{\partial\mathcal{E}}(\mathbf{v}\times\mathbf{B})\cdot\left(\mathbf{Z}+\left(\mathbf{k}\cdot\frac{\partial\mathbf{Z}}{\partial\mathcal{E}}\right)\hbar\mathbf{v}\right)\\
&= \frac{e}{m_n}\frac{\partial f_0}{\partial\mathcal{E}}(\mathbf{v}\times\mathbf{B})\cdot\mathbf{Z}\\
&= \frac{e}{m_n}\frac{\partial f_0}{\partial\mathcal{E}}(\mathbf{B}\times\mathbf{Z})\cdot\mathbf{v}. \qquad (6.25)
\end{aligned}
$$

$$(6.26)$$

In the last of the above equations the following property of the mixed product was used: $\mathbf{A}\cdot(\mathbf{B}\times\mathbf{C})=\mathbf{B}\cdot(\mathbf{C}\times\mathbf{A})$. Using eqs. (6.23,6.24,6.25,6.22, 6.14) in (6.21), one obtains:

$$\mathbf{Z}-\frac{e\tau(\mathbf{k})}{m_n}(\mathbf{B}\times\mathbf{Z})=-e\tau(\mathbf{k})\mathbf{E}. \qquad (6.27)$$

Next we proceed as follows:
- considering the scalar product of (6.27) with $\mathbf{B}$; since $\mathbf{B}\cdot(\mathbf{B}\times\mathbf{Z})=0$, one obtains:

$$\mathbf{B}\cdot\mathbf{Z}=-e\tau(\mathbf{k})\mathbf{B}\cdot\mathbf{E}; \qquad (6.28)$$

- considering the vectorial product of (6.27) with $\mathbf{B}$ to the left and using the algebraic identity $\mathbf{A}\cdot(\mathbf{B}\times\mathbf{C})=\mathbf{B}(\mathbf{A}\cdot\mathbf{C})-\mathbf{C}(\mathbf{A}\cdot\mathbf{B})$, one obtains:

$$\mathbf{B}\times\mathbf{Z}-\frac{e\tau(\mathbf{k})}{m_n}(\mathbf{B}(\mathbf{B}\cdot\mathbf{Z})-B^2\mathbf{Z})=-e\tau(\mathbf{k})\mathbf{B}\times\mathbf{E}; \qquad (6.29)$$

Using (6.28) and (6.29) in (6.27) one finaly obtains:

$$\mathbf{Z}=-e\tau(\mathbf{k})\frac{\mathbf{E}+\frac{e\tau(\mathbf{k})}{m_n}\mathbf{B}\times\mathbf{E}+\left(\frac{e\tau(\mathbf{k})}{m_n}\right)^2\mathbf{B}(\mathbf{B}\cdot\mathbf{E})}{1+\left(\frac{e\tau(\mathbf{k})}{m_n}\right)^2B^2}. \qquad (6.30)$$

Sometimes $\mathbf{Z}$ in the above equation is called Hall field. The current through the sample is given by:

$$\mathbf{j}=-e\sum\mathbf{k},sf(\mathbf{k})\mathbf{v}=-e\sum\mathbf{k},sf_1(\mathbf{k})\mathbf{v}, \qquad (6.31)$$

where s is the spin projection quantum number. In establishing the last form of eq. (6.31), the expression $\sum\mathbf{k},sf_0(\mathbf{k})\mathbf{v}=0$ was considered (the function under the sum sign is anti-symmetric, i.e. $f_0(-\mathbf{k})\mathbf{v}(-\mathbf{k})=-f_0(\mathbf{k})\mathbf{v}$, so, when summing over the first Brillouin zone the result is zero). Passing to integral over the first Brillouin zone (6.31) reads:

$$
\begin{aligned}
\mathbf{j} &= \frac{-2e}{(2\pi)^3}\int_{\mathbf{k}\in BZ}f_1(\mathbf{k})\mathbf{v}d^3k\\
&= \frac{-e}{4\pi^3}\int_{\mathbf{k}\in BZ}(\mathbf{Z}\cdot\mathbf{v})\mathbf{v}\frac{\partial f_0}{\partial\mathcal{E}}d^3k. \qquad (6.32)
\end{aligned}
$$

Observe that if $\mathbf{E}=0$ then $\mathbf{j}=0$: the magnetic field does not give rise to a net chrage flow through the sample. In addition, even if the semiconductor material was assumed to be isotropic in this calculation, eq. (6.32) shows that the conductivity tensor is anisotropic (the current density is not parallel to the electric field), due to the anisotropy induced by the magnetic field.

Conductivity tensor

Let us consider that the magnetic field is oriented along Oz axis, i.e. $\mathbf{B} = (0, 0, B_z)$. The electric field is $\mathbf{E} = (E_x, E_y, E_z)$. Then:

$$\begin{aligned}\mathbf{B} \times \mathbf{E} &= \begin{vmatrix} \mathbf{x} & \mathbf{y} & \mathbf{z} \\ 0 & 0 & B_z \\ E_x & E_y & E_z \end{vmatrix} \\ &= -E_y B_z \mathbf{x} + E_x B_z \mathbf{y}\end{aligned}$$

and (6.30) leads to:

$$\begin{aligned} Z_x(\mathbf{k}) &= -e\tau(\mathbf{k}) \frac{E_x - \omega_c \tau(\mathbf{k}) E_y}{1 + \omega_c^2 \tau^2(\mathbf{k})} \\ Z_y(\mathbf{k}) &= -e\tau(\mathbf{k}) \frac{E_y + \omega_c \tau(\mathbf{k}) E_x}{1 + \omega_c^2 \tau^2(\mathbf{k})} \qquad (6.33) \\ Z_z(\mathbf{k}) &= -e\tau(\mathbf{k}) E_z, \qquad (6.34) \end{aligned}$$

where $\omega_c = \frac{eB}{m_n}$ is cyclotron pulsation. It follows that the density current on Ox direction (see (6.32)) is given by:

$$\begin{aligned} j_x &= \frac{-e}{4\pi^3} \int_{\mathbf{k} \in BZ} (Z_x v_x + Z_y v_y + Z_z v_z) v_x \frac{\partial f_0}{\partial \mathcal{E}} d^3k \\ &= \frac{-e}{4\pi^3} \int_{\mathbf{k} \in BZ} Z_x v_x^2 \frac{\partial f_0}{\partial \mathcal{E}} d^3k \\ &= \frac{e^2 \hbar^2}{6\pi m_n} \int_{k_{min}}^{k_{max}} \left(-\frac{\partial f_0}{\partial \mathcal{E}} \right) \frac{k^4 \tau(\mathbf{k})}{1 + \omega_c^2 \tau^2(\mathbf{k})} (E_x - \omega_c \tau(\mathbf{k}) E_y) dk \\ &= \frac{(2m_n)^{3/2} e^2}{3\pi^2 \hbar^3 m_n} \int_0^{\infty} \left(-\frac{\partial f_0}{\partial \mathcal{E}} \right) \frac{\mathcal{E}^{3/2} \tau(\mathcal{E})}{1 + \omega_c^2 \tau^2(\mathcal{E})} (E_x - \omega_c \tau(\mathcal{E}) E_y) d\mathcal{E}, \qquad (6.35) \end{aligned}$$

where it was assumed that $\mathbf{B}$ is low enough, so that the energy spectrum in the conduction band (6.13) is not changed, and also that $\tau(\mathbf{k}) = \tau(-\mathbf{k})$, so the integrals over Brillouin zone with odd powers of velocity components vanish. Using also the expression for the equilibrium electron density:

$$\begin{aligned} n &= \frac{1}{V} \sum_{\mathbf{k},s} f_0(\mathbf{k}) \\ &= \frac{2}{(2\pi)^3} \int_{\mathbf{k} \in BZ} f_0(\mathbf{k}) d^3k \\ &= \frac{1}{\pi^2} \int_{k_{min}}^{k_{max}} f_0(\mathbf{k}) dk \\ &= \frac{(2m_n)^{3/2}}{2\pi^2 \hbar^3} \int_0^{\infty} f_0(\mathcal{E}) \mathcal{E}^{1/2} d\mathcal{E} \\ &= \frac{(2m_n)^{3/2}}{3\pi^2 \hbar^3} \int_0^{\infty} \left(-\frac{\partial f_0}{\partial \mathcal{E}} \right) \mathcal{E}^{3/2} d\mathcal{E}, \qquad (6.36) \end{aligned}$$

the expression (6.35) reads:

$$j_x = \sigma_{xx} E_x + \sigma_{xy} E_y, \tag{6.37}$$

with:

$$\sigma_{xx} = \frac{ne^2}{m_n} \left\langle \frac{\tau}{1+\omega_c^2\tau^2} \right\rangle \tag{6.38}$$

$$\sigma_{xy} = -\frac{ne^2}{m_n} \left\langle \frac{\omega_c\tau^2}{1+\omega_c^2\tau^2} \right\rangle . \tag{6.39}$$

$$\tag{6.40}$$

In (6.38,6.39) $\langle A \rangle$ is the expression:

$$\langle A \rangle = \frac{\int_0^\infty \left(-\frac{\partial f_0}{\partial \mathcal{E}}\right) A(\mathcal{E}) \mathcal{E}^{3/2} d\mathcal{E}}{\int_0^\infty \left(-\frac{\partial f_0}{\partial \mathcal{E}}\right) \mathcal{E}^{3/2} d\mathcal{E}}, \tag{6.41}$$

which is commonly found in the physics of kinetic phenomena in condensed matter, in Boltzmann's approach.

The same way one finds that:

$$j_y = -\sigma_{xy} E_x + \sigma_{xx} E_y, \tag{6.42}$$

$$j_z = \sigma_{zz} E_z \tag{6.43}$$

with

$$\sigma_{zz} = \frac{ne^2\langle\tau\rangle}{m_n}. \tag{6.44}$$

Consequently, for the analyzed system the conductivity tensor is given by:

$$\hat{\sigma} = \begin{pmatrix} \sigma_{xx} & \sigma_{xy} & 0 \\ -\sigma_{xy} & \sigma_{xx} & 0 \\ 0 & 0 & \sigma_{zz} \end{pmatrix}, \tag{6.45}$$

with components given in (6.38,6.39,6.44).

6.2 Experimental setup and procedure

The experimental setup is shown in Fig.6.2. The module with a monocrystalline germanium test sample is directly connected with the 12 V output of the power unit over the ac-input on the back-side of the module. The Hall voltage and the voltage drop across the sample are measured with a multimeter, using the sockets on the front-side of the module. The current I_x and temperature can be easily read on the integrated display of the module. The magnetic field is measured with the teslameter via a Hall probe, placed in the close vicinity of the germanium sample.

- Set the magnetic field to a value of 250 mT by changing the voltage and current on the power supply. Set the display on the module into the "current-mode". Start the software for measurement configuration and data acquisition and choose Cobra3 as gauge. You will receive first the configuration screen shown in Fig. 6.3. Choose parameters that have to be measured and displayed, e.g. the Hall voltage as a function of the current through the sample. Select all other parameters as shown in Fig. 6.3. Press the "Continue" button. Start the measurement by varying the current through the sample with the "Ip"-knob on the frontside of the module and starting the software.
  Record the Hall voltage as function of the current from -30 mA up to 30 mA. U_H vs. I_x experimental curve shape will be as shown in Fig. 6.4.

Fig. 6.2. Experimental setup for temperature dependent Hall effect measurements.

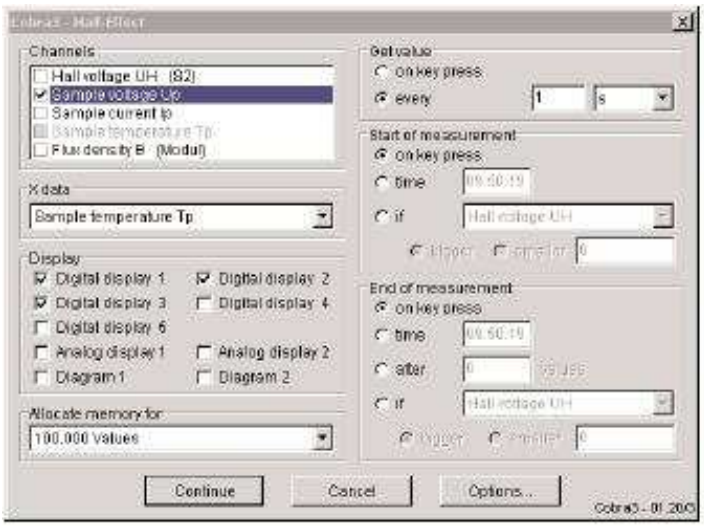

Fig. 6.3. Start menu of the Cobra3 software for measurement configuration and data acquisition.

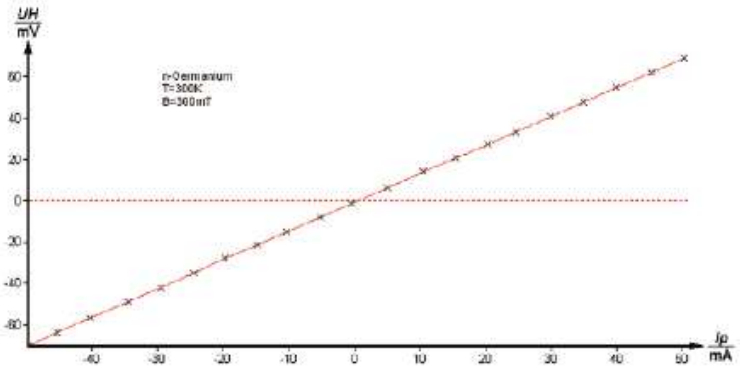

Fig. 6.4. Hall voltage as a function of the current through the sample.

- Set the current to 30 mA. Repeat the above mentioned steps, but configure the measurement to record the Hall voltage as a function of magnetic field. Record the Hall voltage as a function of the (positive) magnetic induction B up to 300 mT.
- Put the display in temperature mode. Set the current to a value of 30 mA. The magnetic field is off. The current is kept constant during the measurement, but the longitudinal voltage changes due to changes in temperature. Configure the measurement to record the Hall voltage as a function of temperature. Start the measurement by activating the heating coil with the "ON/OFF"-knob on the backside of the module and starting the software. Record the temperature dependence of the voltage for a temperature range from the ambient temperature to a maximum of 170°C. The typical $U_x(T)$ dependence is shown in Fig. 6.5; since the current was constant, and $\sigma = \frac{l}{S}\frac{I_x}{U_x}$, l being the length and S the transverse area of the sample, this is essentially a plot of the conductivity as function of the inverse of temperature, in the absence of the magnetic field.

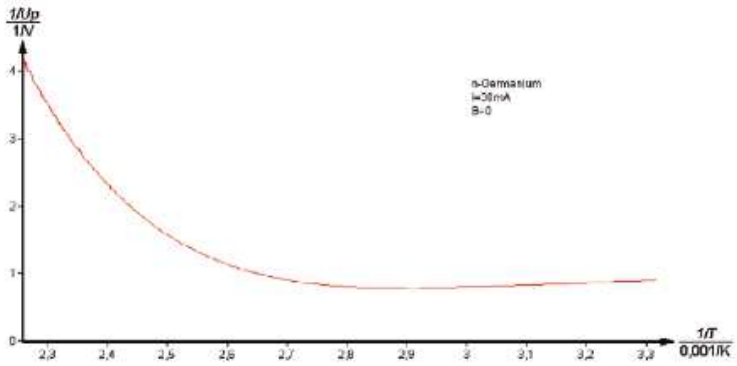

Fig. 6.5. Hall voltage as a function of the current through the sample.

- Set the current to 30 mA and the magnetic induction to 300 mT. Record the Hall voltage as a function of temperature. Set the display in the temperature mode. Start the measurement by activating the heating coil with the "ON/OFF"-knob on the backside of the module and starting the software. The typical $U_H(T)$ dependence is shown in Fig. 6.6.

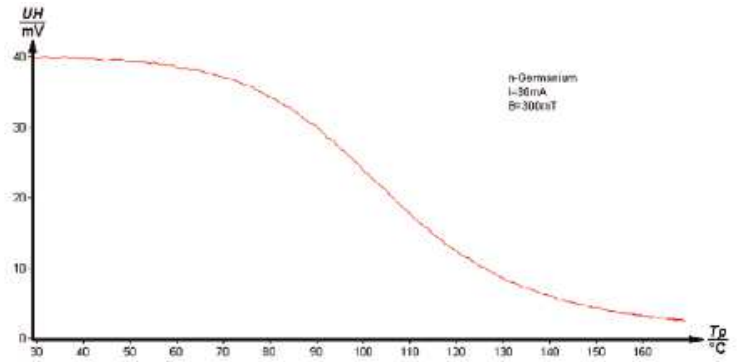

Fig. 6.6. Hall voltage as a function of temperature.

6.3 Tasks

The sample is a rectangular piece of germanium, $20 \times 10 \times 1\,\mathrm{mm}^3$.

- Check that the Hall voltage is proportional to both the current I_x and the magnetic field B, as suggested by eq. (6.2), which can be put into the form:

$$R_H = \frac{U_H d}{I_x B}, \tag{6.46}$$

  with d being the thickness of the sample. Identify the conduction type of the sample.
- Based on the experimental data, calculate and plot $R_H(T)$, $n(T)$ and $\mu_H(T)$, by using eqs. (6.46,6.10,6.12). Comment the results. What is the dominant scattering mechanism?

Boltzmann's constant is $k_B = 8.625 \times 10^{-5}$ eV and the absolute value of the electron charge is $e = 1.602 \times 10^{-19}$ C.

7

Optical absorption in semiconductors

The purpose of this practical work is to study optical absorption in semiconductors near the fundamental absorption threshold and to measure the bandgap.

7.1 Theory

You have already learned that in a perfect semiconductor the ground state at $T = 0\,K$ correspond to completely filled valence bands, while the conduction band is completely empty. All states in allowed energy bands in the energetic spectrum are extended Bloch states. A semiconductor is characterized by the fact that even at non-zero temperatures the valence band is macroscopically filled, while the conduction band is almost empty. Only a small number of states in the vicinity of the minimum energy in the conduction band are filled with electrons at $T \neq 0\,K$, this number depending exponentially on the temperature. Photons with energies above the bandgap of a semiconductor will be absorbed, inducing electron transitions from states in the valence band to states in the conduction band. Due to high densities of states in the two bands, this process may be very intense.
Optical properties of semiconductors strongly depend on the peculiarities of the valence and conduction band dispersion relations $E_{c,v}(\mathbf{k})$. At energies near the maximum of valence band and minimum of conduction band of a semiconductor, two distinct types of dispersion relations can occur (see Fig. 7.1): either the maximum of the valence band and the minimum of conduction band correspond to the same $\mathbf{k}$ in the first Brillouin zone, or they correspond to different $\mathbf{k}$'s. In the first case the semiconductor is called a *direct band gap semiconductor*, while in the second it is called *an indirect band gap semiconductor*. The two types of semiconductors have very different optical responses at photon energies near the bandgap.

ZnO, GaAs, CdS, CdTe are direct band gap semiconductors, while Si and Ge are indirect band gap semiconductors.
Let's start by considering the case of a direct band gap semiconductor. The one-electron Hamiltonian characterising electron states in the crystal is in its simplest form:

$$H_0 = \frac{p^2}{2m} + V(\mathbf{r}), \tag{7.1}$$

where $V(\mathbf{r}) = V(\mathbf{r} + \mathbf{R})$ is the crystalline potential energy, with $\mathbf{R} = n_1\mathbf{a}_1 + n_2\mathbf{a}_2 + n_3\mathbf{a}_3$ any Bravais' vector. We will describe the incident electromagnetic field in the Coulomb gauge, with the scalar potential $\Phi(\mathbf{r}, t) = 0$ and the vectorial potential $\mathbf{A}(\mathbf{r}, t) = A_0\mathbf{e}_p e^{i(\mathbf{q}\cdot\mathbf{r}-\omega t)}$, with $\nabla \cdot \mathbf{A} = 0$, $\mathbf{e}_p$ describing the polarization state of the electromagnetic monochromatic transverse wave with wave-vector $\mathbf{q}$ and pulsation ω. In this gauge the electric and magnetic fields are given by $\mathbf{E} = -\frac{\partial \mathbf{A}}{\partial t}$, $\mathbf{B} = \boldsymbol{\nabla}\mathbf{A}$. Then the expression of the one-electron Hamiltonian in the presence of the field reads:

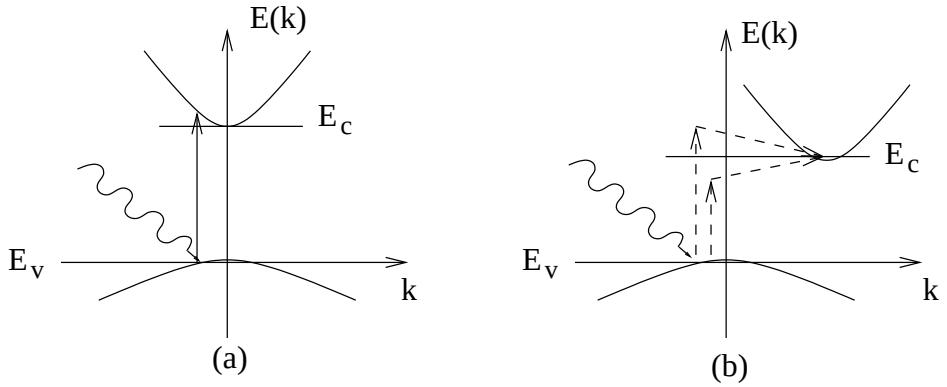

Fig. 7.1. (a) Semiconductor with direct gap: the maximum of the valence band and the minimum of the conduction band occur at the same point **k** in the first Brillouin zone (in this case the center of the Brillouin zone). (b) Semiconductors with indirect gap: the maximum of valence band and the minimum of conduction band occur at different points in the first Brillouin zone.

$$\begin{aligned} H &= \frac{(\mathbf{p}+e\mathbf{A})^2}{2m} + V(\mathbf{r}) \\ &= H_0 + \frac{eA_0}{m} e^{i(\mathbf{q}\cdot\mathbf{r}-\omega t)} \mathbf{e}_p \cdot \mathbf{p} + \frac{e^2\mathbf{A}^2(\mathbf{r},t)}{2m} \\ &= H_0 + H_1 + H_2, \end{aligned} \tag{7.2}$$

where $H_1 = \frac{eA_0}{m} e^{i(\mathbf{q}\cdot\mathbf{r}-\omega t)} \mathbf{e}_p \cdot \mathbf{p}$ and $H_2 = \frac{e^2\mathbf{A}^2(\mathbf{r},t)}{2m}$. The term H_2 in (7.2) is important only if the electromagnetic field is intense (e.g. laser radiation). In the present experimental conditions it can be neglected. In obtaining eq. (7.2) it was taken into account that the commutator $[\mathbf{p}, \mathbf{A}] = -i\hbar\nabla \cdot \mathbf{A}$ is zero in Coulomb gauge, since $\nabla \cdot \mathbf{A} = 0$ (transverse polarized field).

Next we will suppose that the field is weak enough to use the results of the first order time dependent quantum perturbation theory in describing the transition od an electron from an occupied Bloch state in the valence band, $\psi_{v\mathbf{k}_v,\sigma}(\mathbf{r})$, to a free Bloch state in the conduction band, $\psi_{c\mathbf{k}_c,\sigma}(\mathbf{r})$. Following Fermi's golden rule, the probability rate for that single transition to occur is given by:

$$\frac{d\mathcal{P}_{cv}}{dt} = \frac{2\pi}{\hbar} |\langle \psi_{c\mathbf{k}_c,\sigma} | H_{1A} | \psi_{v\mathbf{k}_v,\sigma} \rangle|^2 \delta(E_c(\mathbf{k}_c) - E_v(\mathbf{k}_v) - \hbar\omega) f_0(E_v(\mathbf{k}_v))[1 - f_0(E_c(\mathbf{k}_c))], \tag{7.3}$$

with $H_{1A} = \frac{eA_0}{m} e^{i\mathbf{q}\cdot\mathbf{r}} \mathbf{e}_p \cdot \mathbf{p}$ and $f_0(E) = \frac{1}{1+e^{\frac{E-E_F}{k_B T}}}$ is Fermi-Dirac distribution function. Since the valence band is practically filled and the conduction band is practically empty, Pauli factor is $f_0(E_v(\mathbf{k}_v))[1 - f_0(E_c(\mathbf{k}_c))] \approx 1$ and will be droped in the following.
The matrix element in eq. (7.3) may be transformed as follows:

$$\begin{aligned} \langle \psi_{c\mathbf{k}_c,\sigma} | H_{1A} | \psi_{v\mathbf{k}_v,\sigma} \rangle &= \frac{eA_0}{m} \int_V \psi^*_{\mathbf{k}_c,\sigma}(\mathbf{r}) e^{i\mathbf{q}\cdot\mathbf{r}} \mathbf{e}_p \cdot \mathbf{p} \psi_{\mathbf{k}_v,\sigma}(\mathbf{r}) \\ &= \frac{eA_0}{m} \int_V u^*_{c\mathbf{k}_c,\sigma}(\mathbf{r}) e^{-i\mathbf{k}_c\cdot\mathbf{r}} e^{i\mathbf{q}\cdot\mathbf{r}} \mathbf{e}_p \cdot \mathbf{p} \left(u_{v\mathbf{k}_v,\sigma}(\mathbf{r}) e^{i\mathbf{k}_v\cdot\mathbf{r}} \right) \\ &= \frac{eA_0}{m} \int_V u^*_{c\mathbf{k}_c,\sigma}(\mathbf{r}) e^{-i\mathbf{k}_c\cdot\mathbf{r}} e^{i\mathbf{q}\cdot\mathbf{r}} \mathbf{e}_p \cdot \left(\hbar\mathbf{k}_v u_{v\mathbf{k}_v,\sigma}(\mathbf{r}) e^{i\mathbf{k}_v\cdot\mathbf{r}} - i\hbar e^{i\mathbf{k}_v\cdot\mathbf{r}} \boldsymbol{\nabla} u_{v\mathbf{k}_v,\sigma}(\mathbf{r}) \right). \end{aligned} \tag{7.4}$$

$$\tag{7.5}$$

The first integral in eq. (7.4) is transformed further by writing it as a sum of integrals over all the primitive cells of the crystal indexed by Bravais vector $\mathbf{R}_l$, with $\mathbf{r} = \mathbf{R}_l + \boldsymbol{\rho}_l$:

$$\begin{aligned}\int_V u^*_{c\mathbf{k}_c,\sigma}(\mathbf{r})e^{-i\mathbf{k}_c\cdot\mathbf{r}}e^{i\mathbf{q}\cdot\mathbf{r}}u_{v\mathbf{k}_v,\sigma}(\mathbf{r})e^{i\mathbf{k}_v\cdot\mathbf{r}} &= \sum_l \int_{V_l} u^*_{c\mathbf{k}_c,\sigma}(\mathbf{R}_l+\boldsymbol{\rho}_l)u_{v\mathbf{k}_v,\sigma}(\mathbf{R}_l+\boldsymbol{\rho}_l)e^{i(\mathbf{k}_v+\mathbf{q}-\mathbf{k}_c)\cdot(\mathbf{R}_l+\boldsymbol{\rho}_l)}d^3\rho_l \\ &= \sum_l e^{i(\mathbf{k}_v+\mathbf{q}-\mathbf{k}_c)\cdot\mathbf{R}_l}\int_{V_l} u^*_{c\mathbf{k}_c,\sigma}(\boldsymbol{\rho}_l)u_{v\mathbf{k}_v,\sigma}(\boldsymbol{\rho}_l)e^{i(\mathbf{k}_v+\mathbf{q}-\mathbf{k}_c)\cdot\boldsymbol{\rho}_l}d^3\rho_l \\ &= \int_{V_p} u^*_{c\mathbf{k}_c,\sigma}(\boldsymbol{\rho})u_{v\mathbf{k}_v,\sigma}(\boldsymbol{\rho})e^{i(\mathbf{k}_v+\mathbf{q}-\mathbf{k}_c)\cdot\boldsymbol{\rho}}d^3\rho\sum_l e^{i(\mathbf{k}_v+\mathbf{q}-\mathbf{k}_c)\cdot\mathbf{R}_l} \\ &= \delta(\mathbf{k}_v+\mathbf{q}-\mathbf{k}_c)NV_p\frac{1}{V_p}\int_{V_p} u^*_{c\mathbf{k}_c,\sigma}(\boldsymbol{\rho})u_{v\mathbf{k}_v,\sigma}(\boldsymbol{\rho})d^3\rho \\ &= 0. \end{aligned} \tag{7.6}$$

In establishing the last result, we have taken into account that the "amplitudes" $u_{\mathbf{k}}(\mathbf{r})$ of Bloch functions are periodic, i.e. $u_{\mathbf{k},\sigma}(\boldsymbol{\rho}+\mathbf{R}_l)=u_{\mathbf{k},\sigma}(\boldsymbol{\rho})$, $\forall\mathbf{R}_l$, and orthonormal, i.e. $\frac{1}{V_p}\int_{V_p} u^*_{n\mathbf{k}_1,\sigma}(\boldsymbol{\rho})u_{n'\mathbf{k}_2,\sigma'}(\boldsymbol{\rho})d^3\rho=\delta_{nn'}\delta_{\sigma\sigma'}\delta(\mathbf{k}_1-\mathbf{k}_2)$, and that $\sum_l e^{i(\mathbf{k}_1-\mathbf{k}_2)\cdot\mathbf{R}_l}=N\delta(\mathbf{k}_1-\mathbf{k}_2)$ with N the number of primitive cells of the crystal. V_p is the volume of the primitive cell.
Applying the same procedure for the second integral in eq. (7.4), one obtains:

$$\begin{aligned}\langle\psi_{c\mathbf{k}_c,\sigma}|H_{1A}|\psi_{v\mathbf{k}_v,\sigma}\rangle &= -i\frac{e\hbar A_0}{m}N\delta(\mathbf{k}_v+\mathbf{q}-\mathbf{k}_c)\int_{V_p} u^*_{c\mathbf{k}_c,\sigma}(\mathbf{r})\mathbf{e}_p\cdot\boldsymbol{\nabla}u_{v\mathbf{k}_v,\sigma}(\mathbf{r})d^3r. \\ &= -i\frac{e\hbar A_0}{m}V\delta(\mathbf{k}_v+\mathbf{q}-\mathbf{k}_c)P_{cv}(\mathbf{k}_c,\mathbf{k}_v),\end{aligned} \tag{7.7}$$

with $P_{cv}(\mathbf{k}_c,\mathbf{k}_v)=\frac{1}{V_p}\int_{V_p} u^*_{c\mathbf{k}_c,\sigma}(\mathbf{r})\mathbf{e}_p\cdot\boldsymbol{\nabla}u_{v\mathbf{k}_v,\sigma}(\mathbf{r})d^3r=\langle u_{c\mathbf{k}_c,\sigma}|\mathbf{e}_p\cdot\boldsymbol{\nabla}|u_{v\mathbf{k}_v,\sigma}\rangle_{V_p}$.
A typical value for the incident monochromatic visible light wave-vector is $q=\frac{2\pi}{\lambda}\approx 10^7$ m^{-1} for $\lambda=500$ nm, while typical values for $k_{c,v}$ in the first Brillouin zone are $\frac{\pi}{a}\approx 10^{10}$ m^{-1} for a lattice constant $a=3.5\mathring{A}$. Since $q\ll k_{c,v}$ it follows that $\mathbf{k}_v+\mathbf{q}\approx\mathbf{k}_v=\mathbf{k}_c$ in eq. (7.7), i.e. the transitions are "vertical" in this case (electron wave-vector $\mathbf{k}$ is conserved in the transition valence band - conduction band in a semiconductor with direct band gap), as suggested in Fig. 7.1a.

The power lost by the incident electromagnetic field due to absorption in unit volume of the crystal is expressed as:

$$\begin{aligned}\hbar\omega\sum_{\mathbf{k}_c,\mathbf{k}_v}\frac{d\mathcal{P}_{cv}}{dt} &= 2\pi\omega\left(\frac{e\hbar A_0}{m}\right)^2\sum_{\mathbf{k}_c,\mathbf{k}_v}|P_{cv}(\mathbf{k}_c,\mathbf{k}_v)|^2\delta(\mathbf{k}_v-\mathbf{k}_c)\delta(E_c(\mathbf{k}_c)-E_v(\mathbf{k}_v)-\hbar\omega) \\ &= 2\pi\omega\left(\frac{e\hbar A_0}{m}\right)^2\sum_{\mathbf{k}}|P_{cv}(\mathbf{k})|^2\delta(E_c(\mathbf{k})-E_v(\mathbf{k})-\hbar\omega) \\ &= \frac{\omega}{(2\pi)^2}\left(\frac{e\hbar A_0}{m}\right)^2\int_{BZ}|P_{cv}(\mathbf{k})|^2\delta(E_c(\mathbf{k})-E_v(\mathbf{k})-\hbar\omega)d^3k \\ &= \frac{\omega}{(2\pi)^2}\left(\frac{e\hbar A_0}{m}\right)^2|P_{cv}|^2\int_{BZ}\delta(E_c(\mathbf{k})-E_v(\mathbf{k})-\hbar\omega)d^3k. \end{aligned} \tag{7.8}$$

$$\tag{7.9}$$

In writing the last line of the above equations it was used the fact that in most cases the matrix element $P_{cv}(\mathbf{k})$ depends slowly on $\mathbf{k}$. The energy flux density of the incident electromagnetic wave is given by the Poynting vector:

$$\mathbf{S}=\frac{1}{\mu_0}\mathbf{E}\times\mathbf{B}=\frac{n\omega^2}{c}A_0^2\mathbf{e}_p\times\frac{\mathbf{q}}{q}e^{i(\mathbf{q}\cdot\mathbf{r}-\omega t)}. \tag{7.10}$$

Combining eqs. (7.8,7.10), *the absorption coefficient* can be defined as:

$$\begin{aligned}\alpha &= \frac{\hbar\omega}{|\mathbf{S}|}\sum_{\mathbf{k}_c,\mathbf{k}_v}\frac{d\mathcal{P}_{cv}}{dt}\\ &= \frac{c}{(2\pi)^2 n\omega}\left(\frac{e\hbar}{m}\right)^2|P_{cv}|^2\int_{BZ}\delta(E_c(\mathbf{k})-E_v(\mathbf{k})-\hbar\omega)d^3k\\ &= \frac{\alpha_0}{\omega}\int_{BZ}\delta(E_c(\mathbf{k})-E_v(\mathbf{k})-\hbar\omega)d^3k\\ &= \frac{\alpha_0}{\hbar\omega}\oiint\limits_{S_{\mathbf{k}}(\omega)}\frac{dS_{\mathbf{k}}}{|\boldsymbol{\nabla}_{\mathbf{k}}E_{cv}(\mathbf{k})|_{S_{\mathbf{k}}(\omega)}}, \qquad (7.11)\end{aligned}$$

(7.12)

where $S_{\mathbf{k}}(\omega)$ is the surface defined in the reciprocal space by $E_{cv}(\mathbf{k}) = E_c(\mathbf{k}) - E_v(\mathbf{k}) = \hbar\omega$ and the following property of Dirac delta generalized function was used:

$$\int f(\mathbf{x})\delta(g(\mathbf{x})) = \oiint\limits_{g(\mathbf{x})=0}\frac{f(\mathbf{x})d\sigma}{|\boldsymbol{\nabla}g(\mathbf{x})|_{g(\mathbf{x})=0}}. \qquad (7.13)$$

The quantity

$$g_{opt}(\omega) = \frac{2}{(2\pi)^3}\oiint\limits_{S_{\mathbf{k}}(\omega)}\frac{dS_{\mathbf{k}}}{|\boldsymbol{\nabla}_{\mathbf{k}}E_{cv}(\mathbf{k})|_{S(\omega)}} \qquad (7.14)$$

appearing in eq. (7.11) is called *joint density of states*. Suppose the dispersion laws in the conduction and valence band are isotropic, given by:

$$E_c(\mathbf{k}) = E_c + \frac{\hbar^2k^2}{2m_n} \qquad (7.15)$$

$$E_v(\mathbf{k}) = E_v - \frac{\hbar^2k^2}{2m_p}. \qquad (7.16)$$

Then the surface $S_{\mathbf{k}}(\omega)$ is a sphere of radius $k = \left(\frac{2m_r}{\hbar^2}\right)^{1/2}(\hbar\omega - E_g)^{1/2}$ and the joint density of state is:

$$g_{opt}(\omega) = \frac{1}{(\pi)^2}\left(\frac{2m_r}{\hbar^2}\right)^{3/2}(\hbar\omega - E_g), \qquad (7.17)$$

where m_r is the reduced mass ($m_r^{-1} = m_n^{-1} + m_p^{-1}$), $E_g = E_c - E_v$ is the (direct) band gap and $\hbar\omega \geq E_g$.

Consequently, replacing the joint density of states in (7.11), the dependence of the optical absorption coefficient on the energy of incident light in the case of a semiconductor with direct bandgap is:

$$\alpha(\omega) = \alpha_0\frac{(\hbar\omega - E_g)^{1/2}}{\hbar\omega}, \qquad (7.18)$$

if $\hbar\omega \geq E_g$.

Eq. (7.18) is used in optical absorption spectroscopy to experimentally measure the bandgap of direct band gap semiconductors.

7.2 Experimental setup and procedure

The experimental setup is shown schematically in Fig.7.2. The white light produced by an incandescent lamp S is fed into the entrance slit of the monochromator MC. The semiconductor sample P (a thin film of CdS

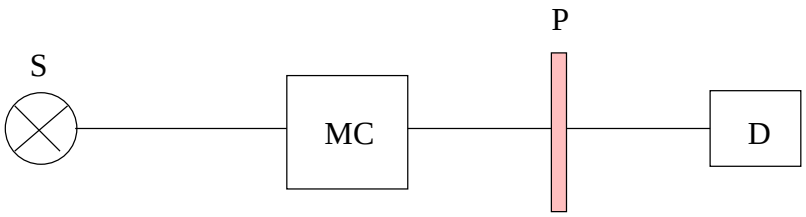

Fig. 7.2. Experimental setup for measurements of the optical absorption coefficient.

deposited on optical glass substrate) is placed at the output slit of the monochromator, in front of the detector D (a Si p-i-n diode).

The response of the detector will be recorded in the wavelength range 800 nm - 500 nm, with and without the semiconductor sample inserted in place. In the range 600 nm - 500 nm use the finest λ-steps allowed by the experimental setup.

7.3 Tasks

- Evaluate the absorbance as $A = \ln \frac{i_0(\lambda)}{i(\lambda)}$, where $i_0(\lambda)$ is the intensity detected at wavelength λ without the semiconductor sample and $i(\lambda)$ is the intensity detected at wavelength λ with the semiconductor sample in place. $A = \alpha d$, where α is the optical absorption coefficient and d is the thickness of the film.
- Plot the quantity $(A\hbar\omega)^2$ against the energy of incident photons $\hbar\omega = \frac{hc}{\lambda}$ ($c = 3 \times 10^8$ m/s is the speed of light). With $h = 6.626 \times 10^{-34}$ J.s the energy of incident photons may be evaluated in eV as:

$$\hbar\omega\,[\text{eV}] = \frac{1242}{\lambda\,[\text{nm}]}. \tag{7.19}$$

  Compare with eq. (7.18) and suggest a method to determine the bandgap E_g. Evaluate the bandgap of CdS.